constricted parts are correlated with distribution of the Triassic. That is, the same as Bou Khil prospect, the high gravity lies regionally in and around the diapir, however the diapir itself is considered to be rock bodies with low density which give rise to low gravity anomaly. Such characteristics are also observed in the first vertical derivative plan. A contour line of 0 mgal/km indicates the boundary between the Cretaceous and Triassic systems and distributions of the Triassic are outlined as an arrangement of low anomalies with extremely small scale.

The mineralized zones of the El Akhouat and the Argoub-Adama are located in and around the jut of high gravity residual. However, both zones can be also considered to be located in and around the constricted parts of the local gravity low with the directions of the NW-SE and E-W. A combination of high and low gravity anomalies indicating density boundary with the NW-SE direction is also observed in the first vertical derivative plan.

4.3.3 IP Survey

Characteristics of IP survey results are described below.

(1) Apparent Resistivity and Observed Chargeability

Apparent resistivity obtained in the El Akhouat prospect is ranging between 0.6 and 471 Ωm and its average is about 80 Ωm which is higher than that obtained in the Bou Khil prospect. The high apparent resistivity zone with the NNE-SSW direction is distributed extending from the central parts to the southern parts of the survey area. The low apparent resistivity zones are distributed in the northern parts, eastern and western ends. The old mine site of El Akhouat is situated in and around the low apparent resistivity anomaly.

Observed chargeability with a maximum value of 47mV/V is generally higher than that obtained in the Bou Khil prospect. The anomalous zones of observed chargeability exceeding 10mV/V are distributed in the old mine site of El Akhouat and extending widely from the central to southern parts of the survey area associated with high apparent resistivity zone. Considering above, the observed chargeability is expected to be an important indicator related with the mineralization. However, the high chargeability is not detected in the vicinity of the old tunnel site of the Argoub Adama, where the useful data have not always been obtained in the low apparent resistivity zone widely distributed in the northern parts of the survey area.

Brief characteristics observed in the cross sections and plans drawn from the IP results are described below.

① Cross Section L0 (Figure 98)

The cross section, connecting between the old tunnel site of Argoub Adama and the old mine site of El Akhouat, runs longitudinally the survey site from the SSW to NNE directions. The zone of high apparent resistivity exceeding 30 Ωm is widely distributed in the southwestern parts from near the station L0-210 and the zone of low apparent resistivity less than 10 Ωm is distributed in the northwestern side. The zone of high apparent resistivity exceeding 100 Ωm with the center around a ridge of the hill lies extending between the stations L0-10 and L0-100 in the south-southwestern side of the section near old mine site of the El Akhouat. The old tunnel site of the Argoub-Adama is situated around the low apparent resistivity zone less than 10 Ωm near the station L0-250.

The chargeability anomaly with 10mV/V, observed in and around the stations L0-10 and L0-110, is associated with the high apparent resistivity anomaly in the south-southwestern side of the section. The chargeability anomaly exceeding 10mV/V in the central parts of the section is observed at lower parts in and around the stations L0-170 and L0-220. The chargeability anomaly is not detected in the vicinity of the old tunnel site of the Argoub Adama, where the useful data have not been obtained because of the low apparent resistivity.

② Cross Section L3 (Figure 99)

The cross section runs through the old mine site of the El Akhouat from the NW to SE directions. The zone of high apparent resistivity exceeding 100 Ωm is widely distributed around the stations from L3-40 through -80 in the central parts of the section. The old mine site of the El Akhouat is situated in the transition zone of the apparent resistivity, where the apparent resistivity is decreasing from the central parts of the high zone towards the southeastern parts.

The strong anomalies of high chargeability exceeding 10mV/V with an anomaly pattern inclining to northwestwards are observed in the vicinity of the old mine site of the El Akhouat. This anomaly lies at the southeastern edge of the high apparent resistivity zone distributed in the central parts of the section.

③ Cross Section L5 (Figure 100)

The cross section runs through north-northeast side parallel to the line L3 with 500m spacing. An anomalous pattern of high apparent resistivity exceeding 100 Ωm is observed at shallow parts in and around the stations L5-40 through -70 in the central parts of the section. This high apparent resistivity anomaly is relatively weak and small compared with that in the section L3 and is changing to the low apparent resistivity less than 30 Ωm at lower parts in the southeastern side. The anomaly pattern of high chargeability exceeding 10mV/V is observed at the lower parts in the central section, where the high apparent resistivity anomaly lies.

④ Cross Section L6 (Figure 101)

The cross section, which is situated at the central parts of the survey area, runs through north-northeast side parallel to the line L5 with 250m spacing. The high anomaly of apparent resistivity exceeding 100 Ωm is observed at shallow parts in and around the stations L6-10 through -125 in the northwestern parts of the section. The low zone of apparent resistivity less than 30 Ωm lying between the stations L6-70 and L6-90 extends to the lower parts of that high apparent resistivity anomaly.

The chargeability anomaly exceeding 10mV/V observed in and around the stations L6-10 through -30 in the northwestern parts of the section extends towards the lower parts in and around stations L6-30 through -60. Especially, the strong chargeability anomaly exceeding 30mV/V is detected at lower parts near the station L6-40.

⑤ Cross Section L7 (Figure 102)

The cross section runs through north-northeast side parallel to the line L6 with 250m spacing. The high anomaly of apparent resistivity exceeding 100 Ωm is observed at shallow parts in and around the stations L7-30 through -40 in the central section. However, the apparent resistivity distributions of this section indicate entirely low apparent resistivity compared with previous sections L3 through L6. The low anomaly of apparent resistivity less than 10 Ωm is observed at lower parts in and around the high apparent resistivity anomaly.

The chargeability anomaly exceeding 10mV/V is observed at lower parts near the station L7-100 in the southeastern section. The weak anomalous zone of the chargeability exceeding 5mV/V is observed in and around the low chargeability and high apparent resistivity anomalies. However, the chargeability distributions of this section show a tendency to be entirely lower compared with previous sections L3 through L6.

⑥ Cross Section L8 (Figure 103)

The cross section runs through north-northeast side parallel to the line L7 with 250m spacing. The apparent resistivity distributions of this section indicate entirely low apparent resistivity the same as that in the line L7. Only small apparent resistivity anomaly with 100 Ωm lies in shallow parts extending from the stations L8-60 to -80 in the southeastern section. The low apparent resistivity anomalies less than 10 Ωm are observed at lower parts in the northwestern and southeastern sections. The chargeability anomaly exceeding 10mV/V, which is followed by the weak anomaly with 5mV/V and higher, is observed around the station L8-60 in the central parts of section.

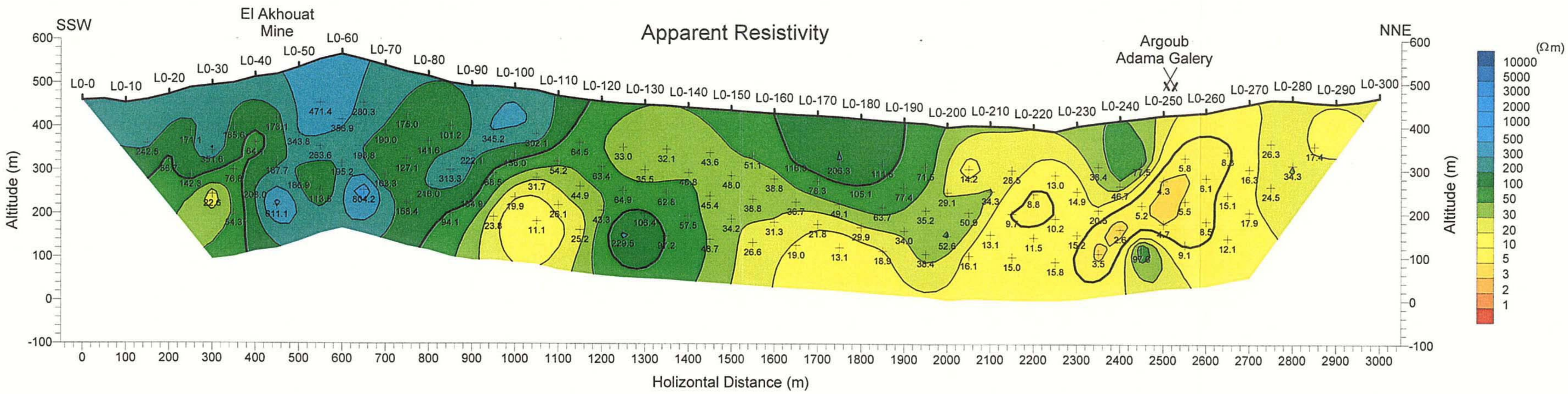

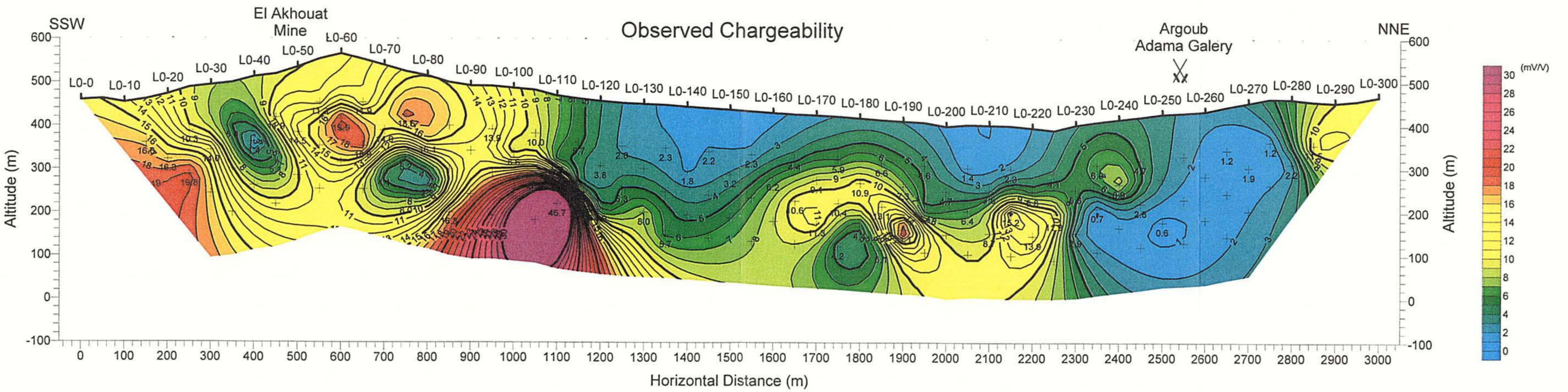

Figure 98 Observed IP section (Line L0)

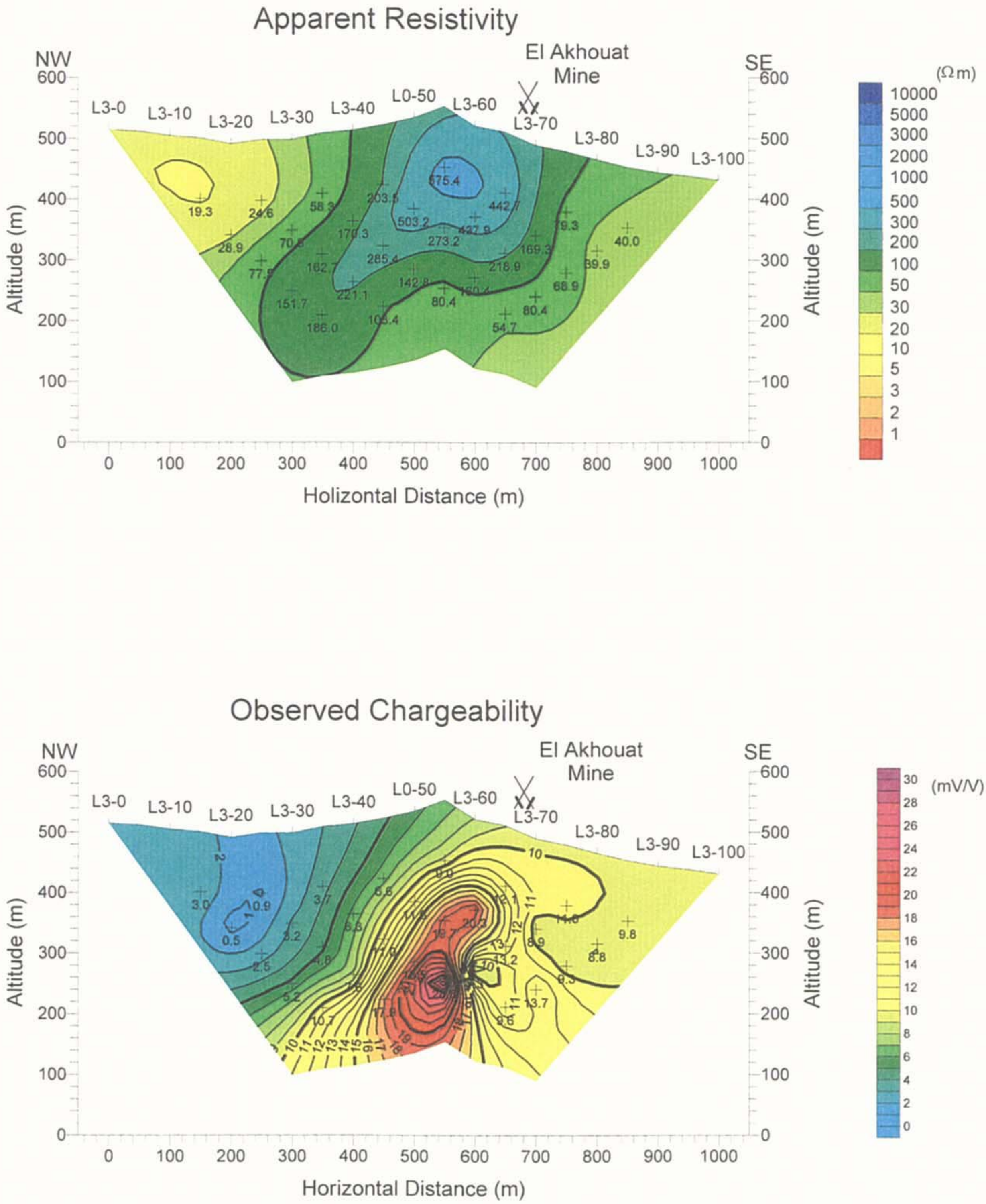

Figure 99 Observed IP cross-section (Line L3)

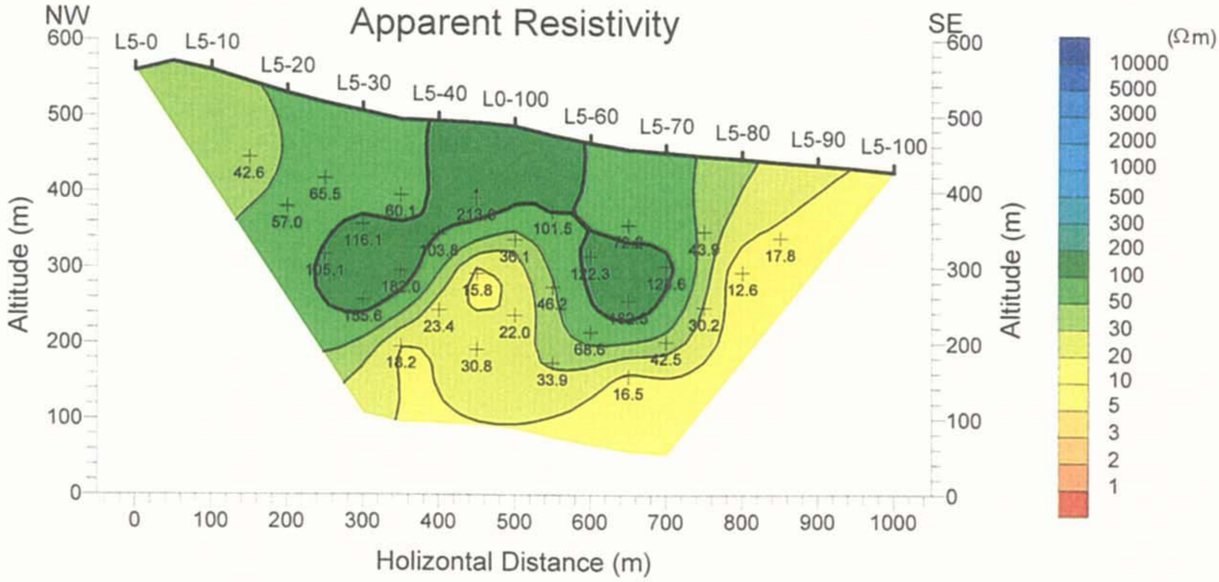

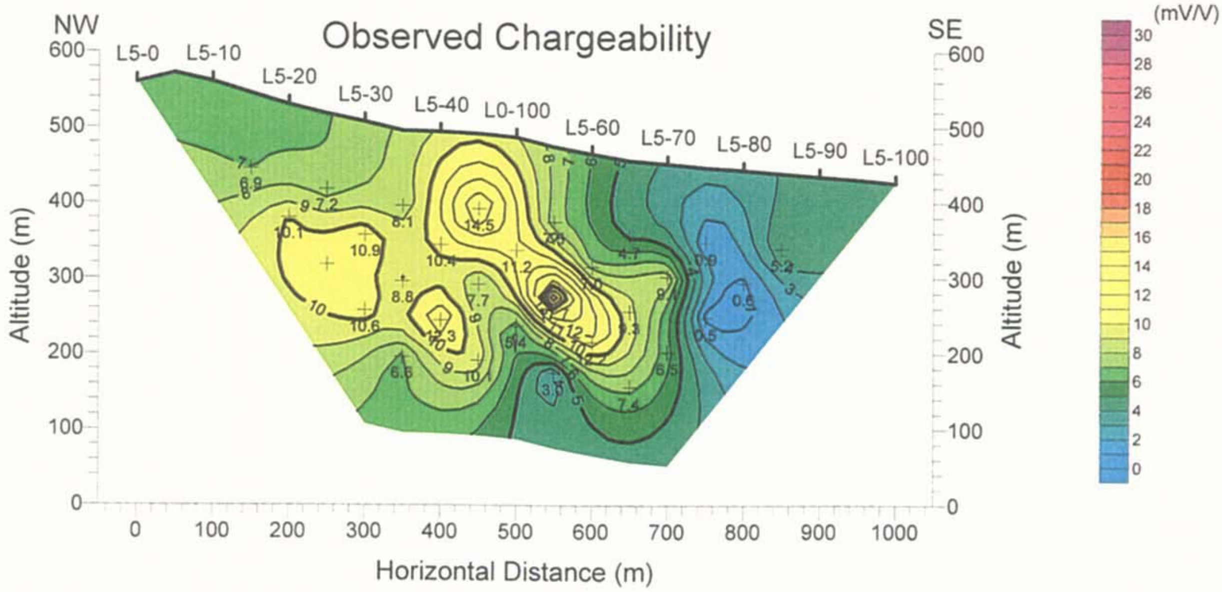

Figure 100 Observed IP cross-section (Line L5)

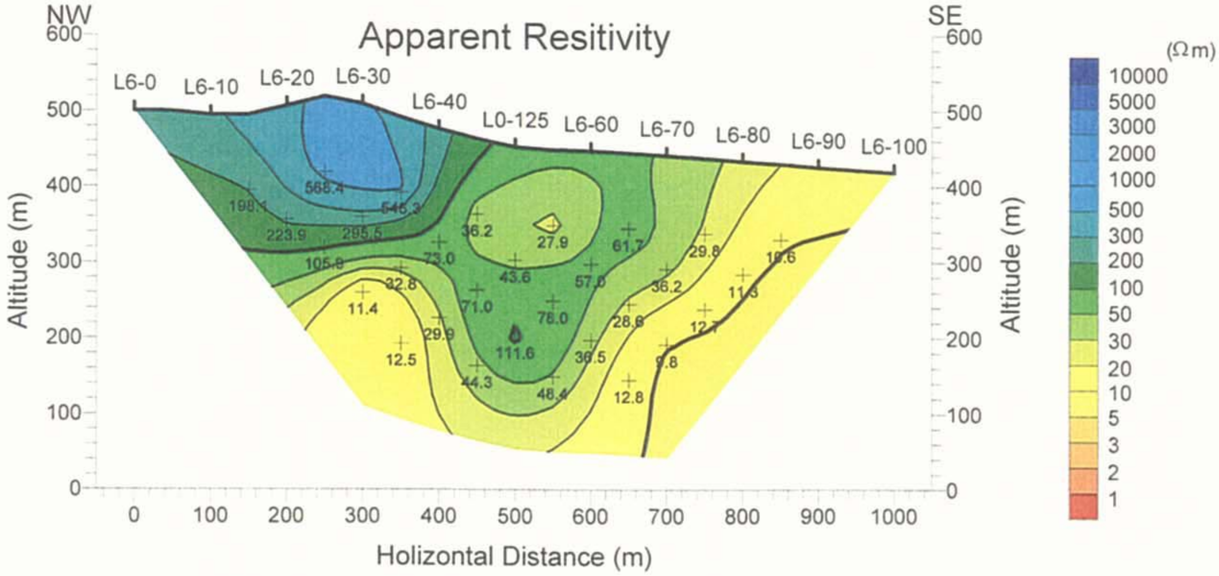

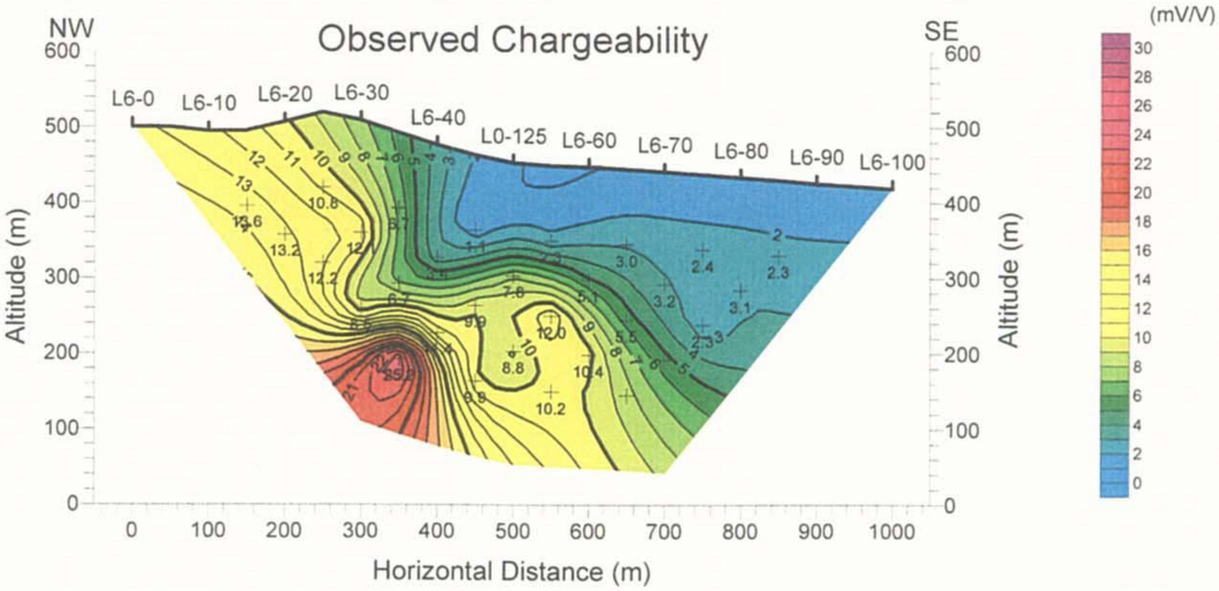

Figure 101 Observed IP cross-section (Line L6)

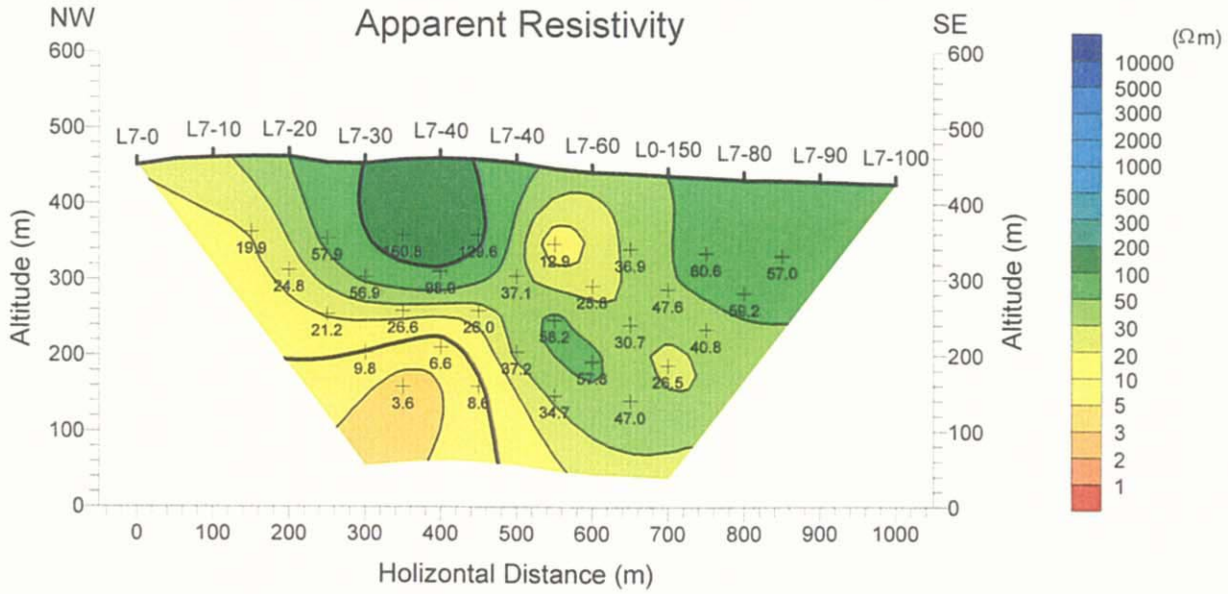

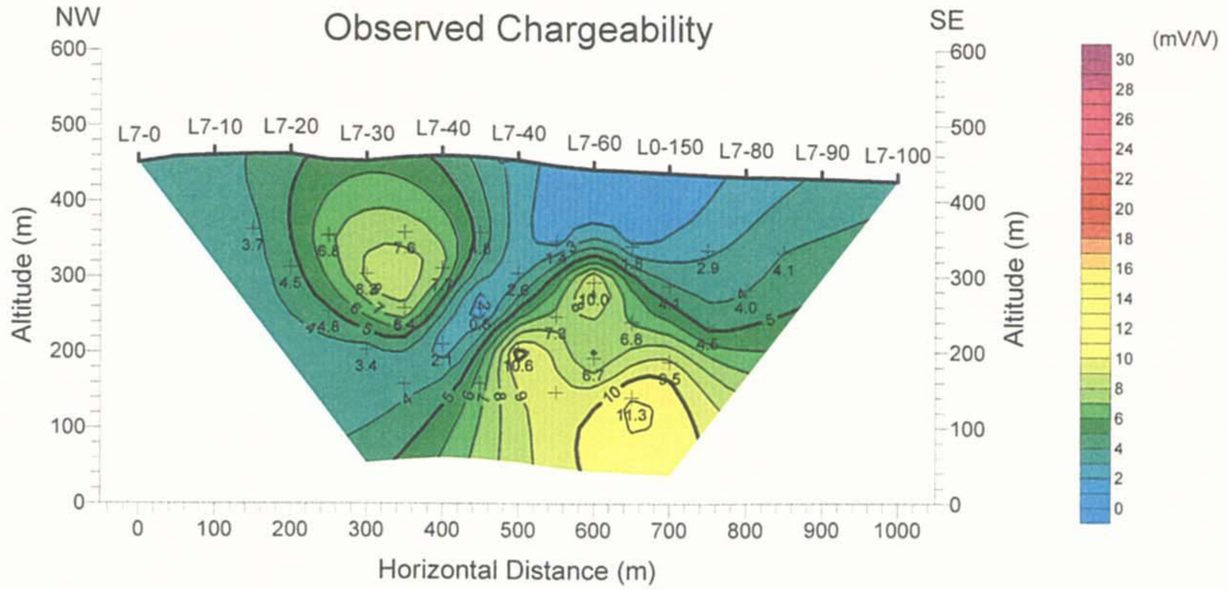

Figure 102 Observed IP cross-section (Line L7)

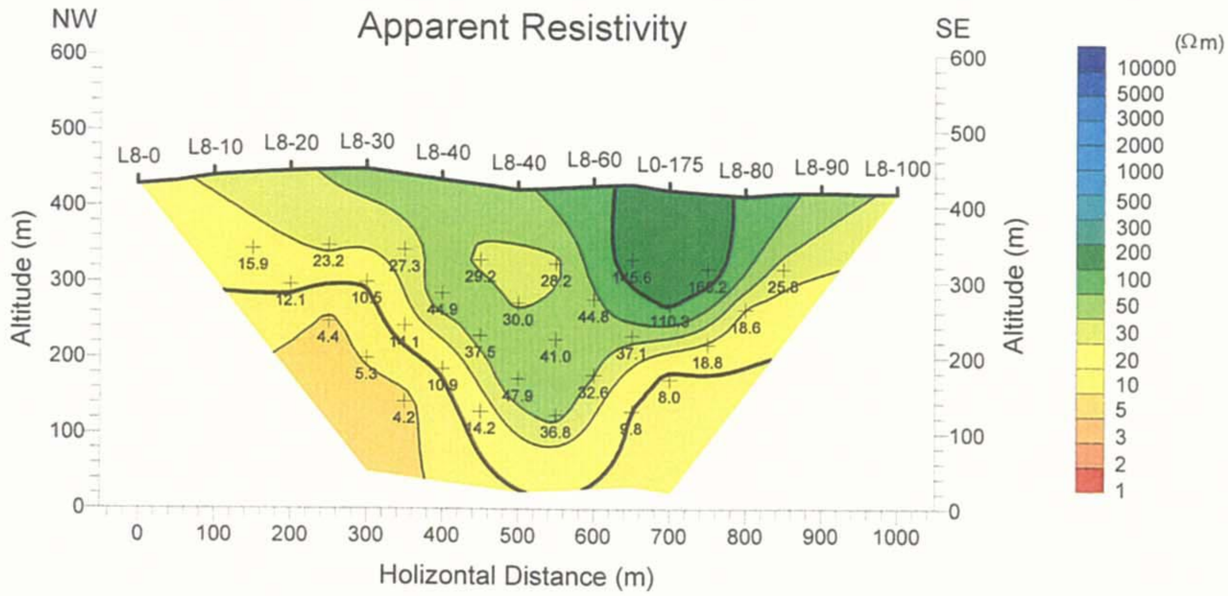

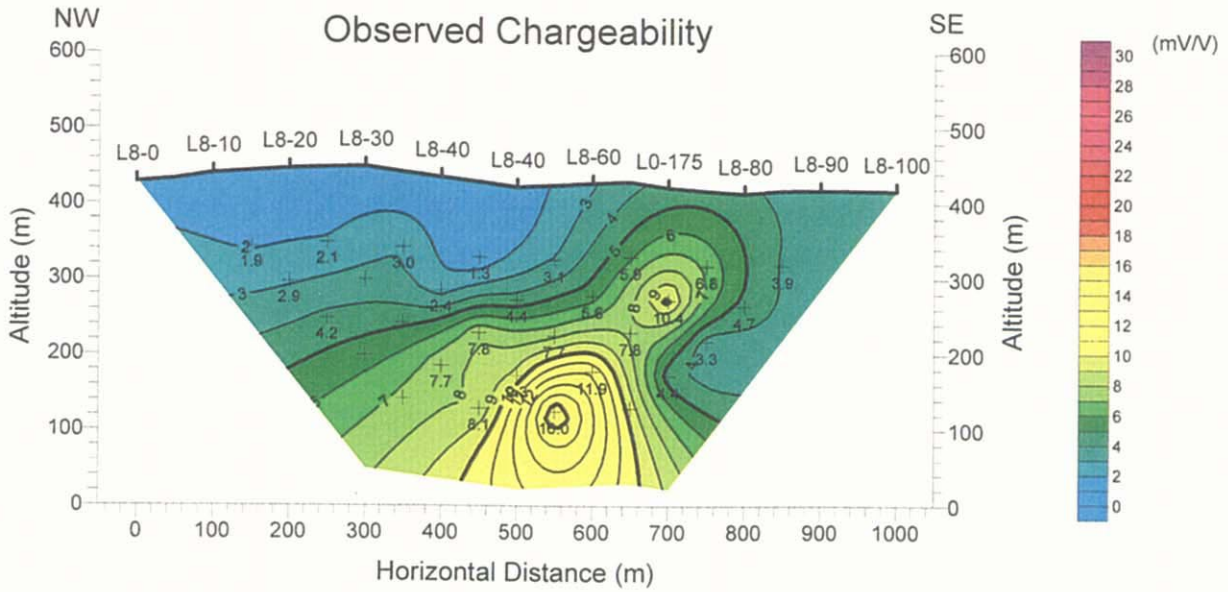

Figure 103 Observed IP cross-section (Line L8)

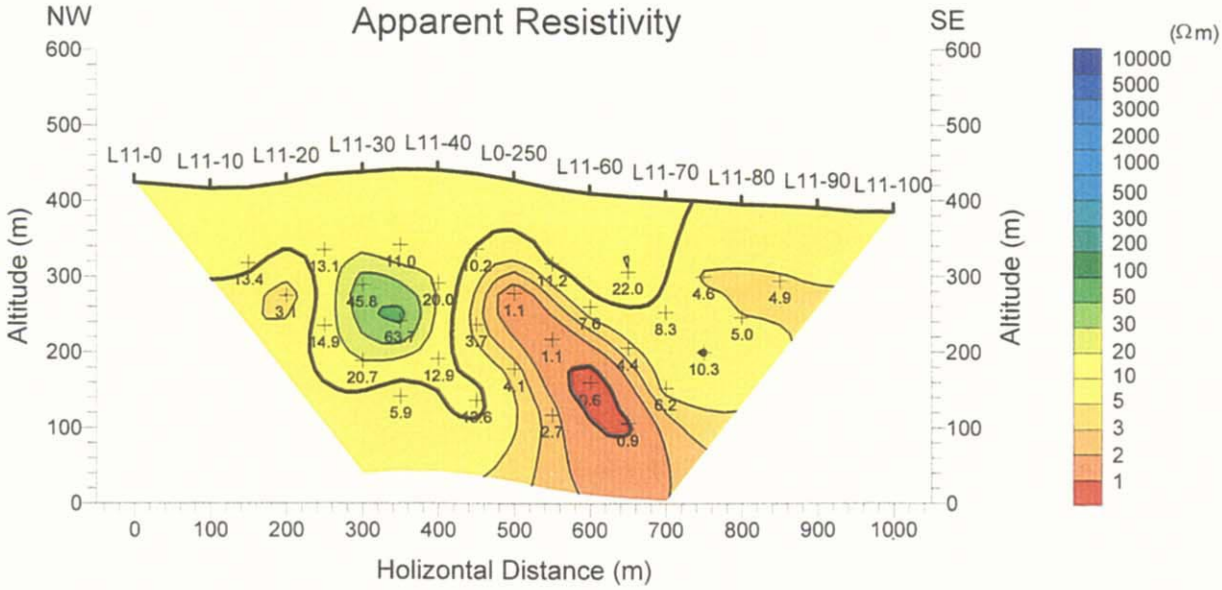

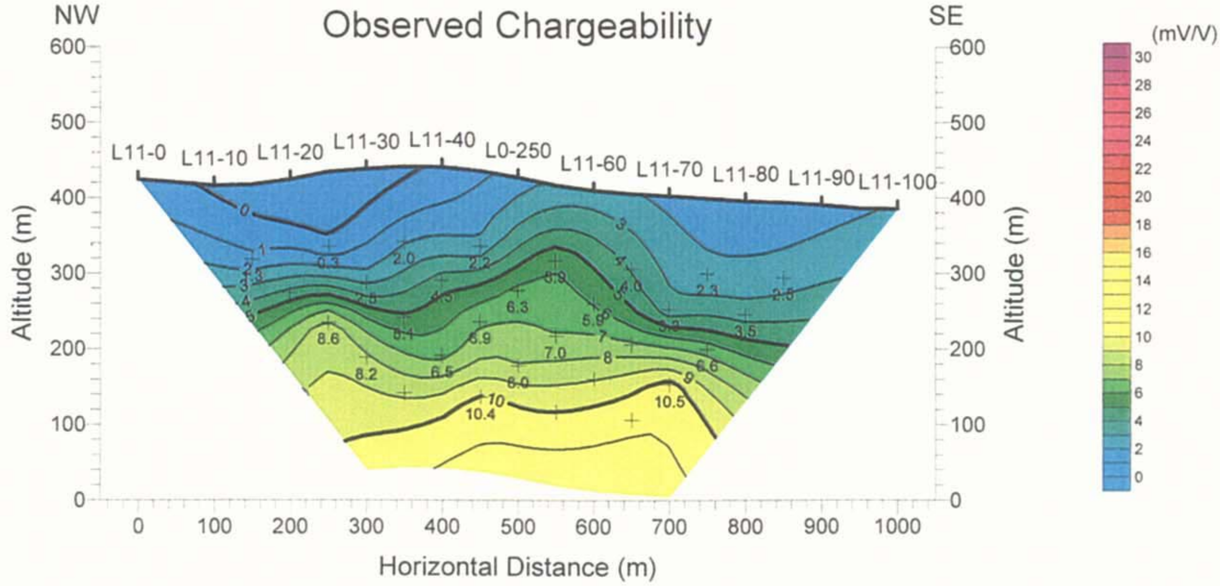

Figure 104 Ovserved IP cross-section (Line L11)

⑦ Cross Section L11 (Figure 104)

The cross section runs through north-northeastern parts of the survey site from the NW to the SE directions. The low zone of apparent resistivity less than 10 Ωm is widely distributed except northwestern parts of the section. The anomalous pattern of the apparent resistivity less than 5 Ωm is observed and extremely low apparent resistivities less than 1Ωm are detected at lower parts around the station L11-60.

The chargeability shows a tendency to become higher extending from the shallower to lower parts and the chargeability anomaly with about 10mV/V is observed.

⑧ Apparent Resistivity Distribution Plan: n=1(Figure 105)

The high apparent resistivity zone exceeding 50 Ωm is distributed extending from the central parts to northwestern parts of the survey area. There are two high apparent resistivity anomalies in the high apparent resistivity zone. One is the anomaly, extending from the station L0-0 to the station L7-40 in the northern parts, indicating the apparent resistivity exceeding 100 Ωm and another one is the anomaly, lying around the station L0-175 in the central parts of the survey area, indicating the apparent resistivity exceeding 100 Ωm. Relatively low apparent resistivity anomalies lie in line cutting the high apparent resistivity anomalies extending from the stations L0-125 to L8-50.

The old mine site of the El Akhouat is located in the eastern edge of the high apparent resistivity extending to the N-S direction. The low apparent resistivities are distributed extending from the northern parts to eastern parts of the survey area and the low apparent resistivity anomaly lies in the vicinity of the old tunnel site of the Argoub-Adama.

⑨ Apparent Resistivity Distribution Plan: n=2(Figure 106)

The apparent resistivity becomes entirely lower compared with that for the previous plan and the low zone of apparent resistivity less than 10 Ωm extends not only to the eastern side but also to the western side in the northern parts of the survey area. The high apparent resistivity anomaly extending from the central parts to the southern parts of the survey area becomes weaker and smaller.

⑩ Apparent Resistivity Distribution Plan: n=3(Figure 107)

The apparent resistivity distributions are generally similar to that for previous two plans and they show a tendency that the apparent resistivities become lower in the northern parts and higher extending from the central parts to the southern parts. Both low anomaly with apparent resistivity less than 10 Ωm in the northern parts of the area and high anomaly in the northern parts of the area become smaller compared with apparent resistivity distribution plans for n=1 and 2.

⑪ Apparent Resistivity Distribution Plan: n=4(Figure 108)

High apparent resistivities become lower and especially an extent, where high apparent resistivities are distributed become considerably smaller and weaker. The distribution extent of the high apparent resistivity anomaly exceeding 100 Ωm extends to the east and west directions. The low zone of apparent resistivity less than 10 Ωm is distributed widely than that for n=3.

⑫ Observed Chargeability Distribution Plan:n=1(Figure 109)

The high chargeability anomaly exceeding 10 mV/V lies extending from near the station L6-20 in the central parts to near the station L3-70 in the southern parts of the survey area. This chargeability anomaly is distributed corresponding to the distribution of the high apparent resistivity anomaly exceeding 100 Ωm. High chargeability anomalies exceeding 10mV/V are observed in the southern and northern ends of the survey area.

The old mine site of the El Akhouat is situated in the high chargeability anomaly exceeding 10mV/V, however the high chargeability anomaly is not detected in the vicinity of the old tunnel site of the Argoub Adama.

⑬ Observed Chargeability Distribution Plan:n=2(Figure 110)

The chargeability distributions extending from the central parts to the southern parts of the survey area are similar as that for n=1. The chargeability anomaly disappears in the northern end and the small chargeability anomaly exceeding 10 mV/V appears around the station L0-175 in the central parts of the survey area.

⑭ Observed Chargeability Distribution Plan:n=3(Figure 111)

The high chargeability anomaly exceeding 10 mV/V extending from the central parts to the southern parts of the survey area, which is indicated on the plans for n=1 and 2, divides into three anomalies distributed around the stations L0-100, L0-50 and L0-10. Maximum values of each anomaly become higher. The chargeability anomaly exceeding 10 mV/V appears around the stations L0-180 and L0-200 extending from the central parts to the northern parts of the survey area.

⑮ Observed Chargeability Distribution Plan:n=4(Figure 112)

The chargeability anomalies exceeding 10 mV/V lie in line around the station L0-50 in the southern parts, the station L0-110 in the central parts and the station L0-280 along the base line L0.

(2) Resistivity and Chargeability Analysis

Analyzed resistivity in the El Akhouat prospect is ranging between 0.4 and 1,771 Ωm and its average is about 70 Ωm. Resistivity structure in this area is generally

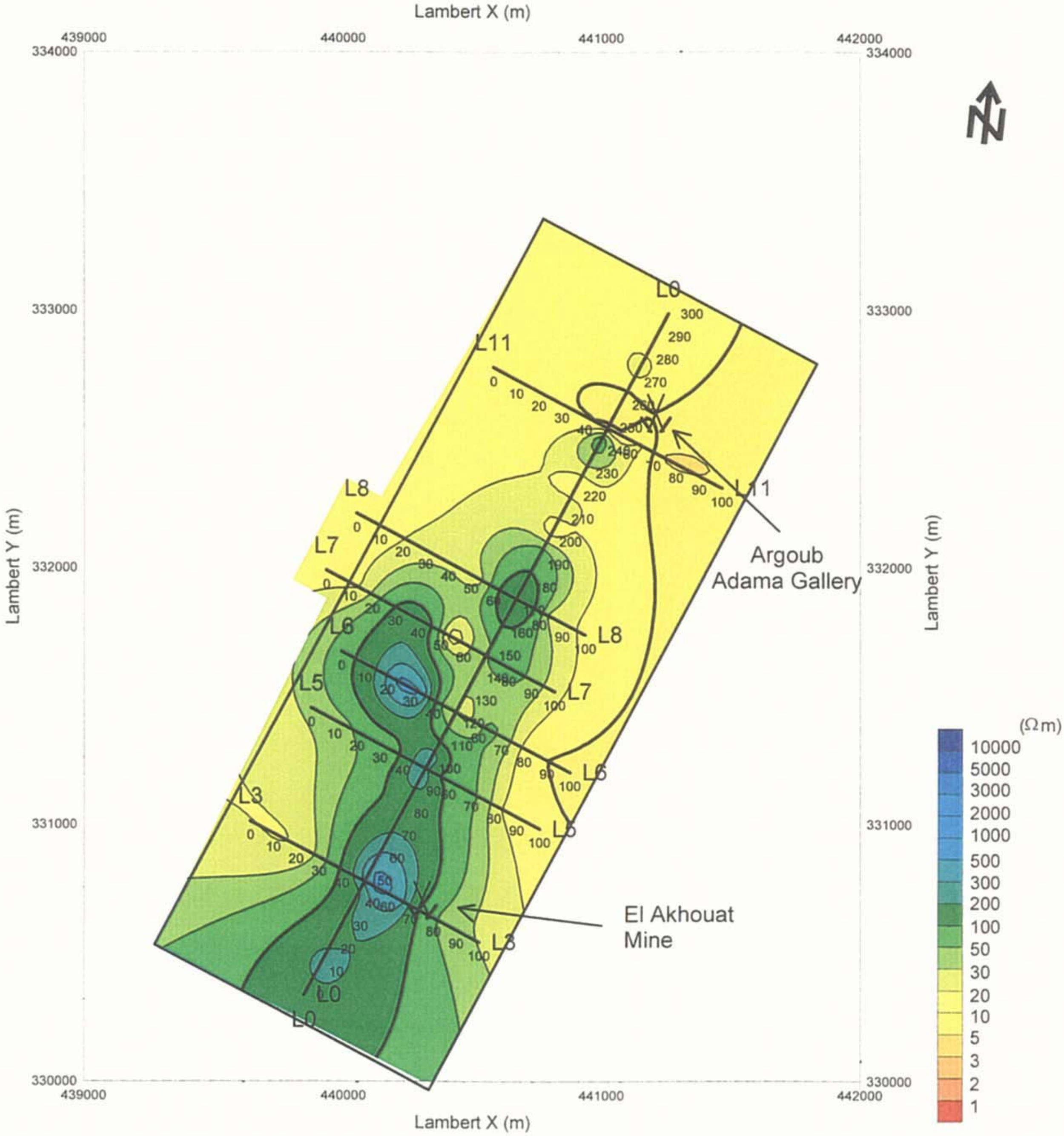

Legend

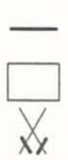

Figure 105
Plan Map of Apparent Resistivity in El Akhouat - Argoub Adama area (n=1)
Scale 1 : 25,000
March, 2000

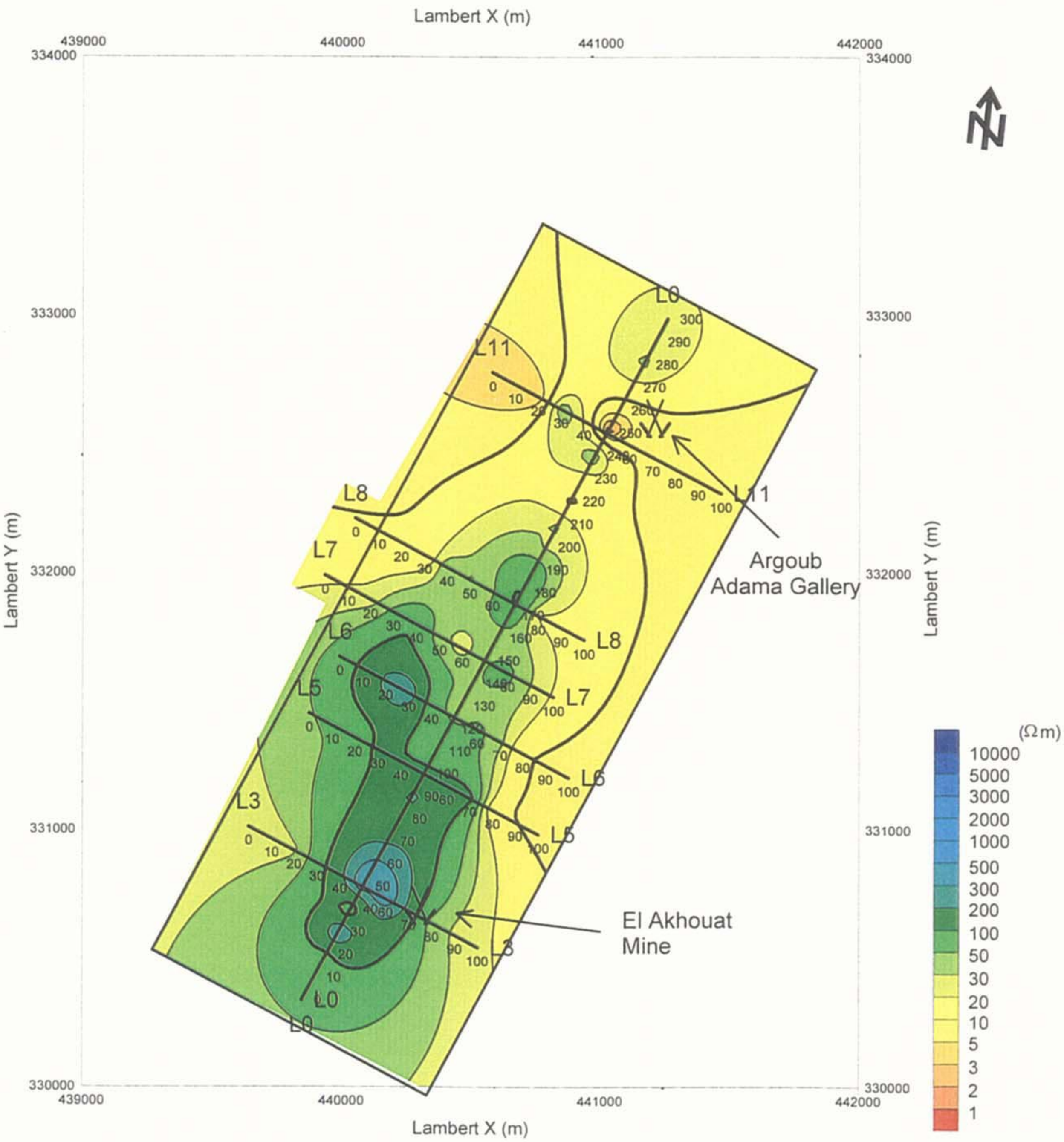

Legend

- : IP survey Line
- : Survey Area
- : Closed Mine

Figure 106

Plan Map of Apparent Resistivity in El Akhouat - Argoub Adama area (n=2)

Scale 1 : 25,000

March, 2000

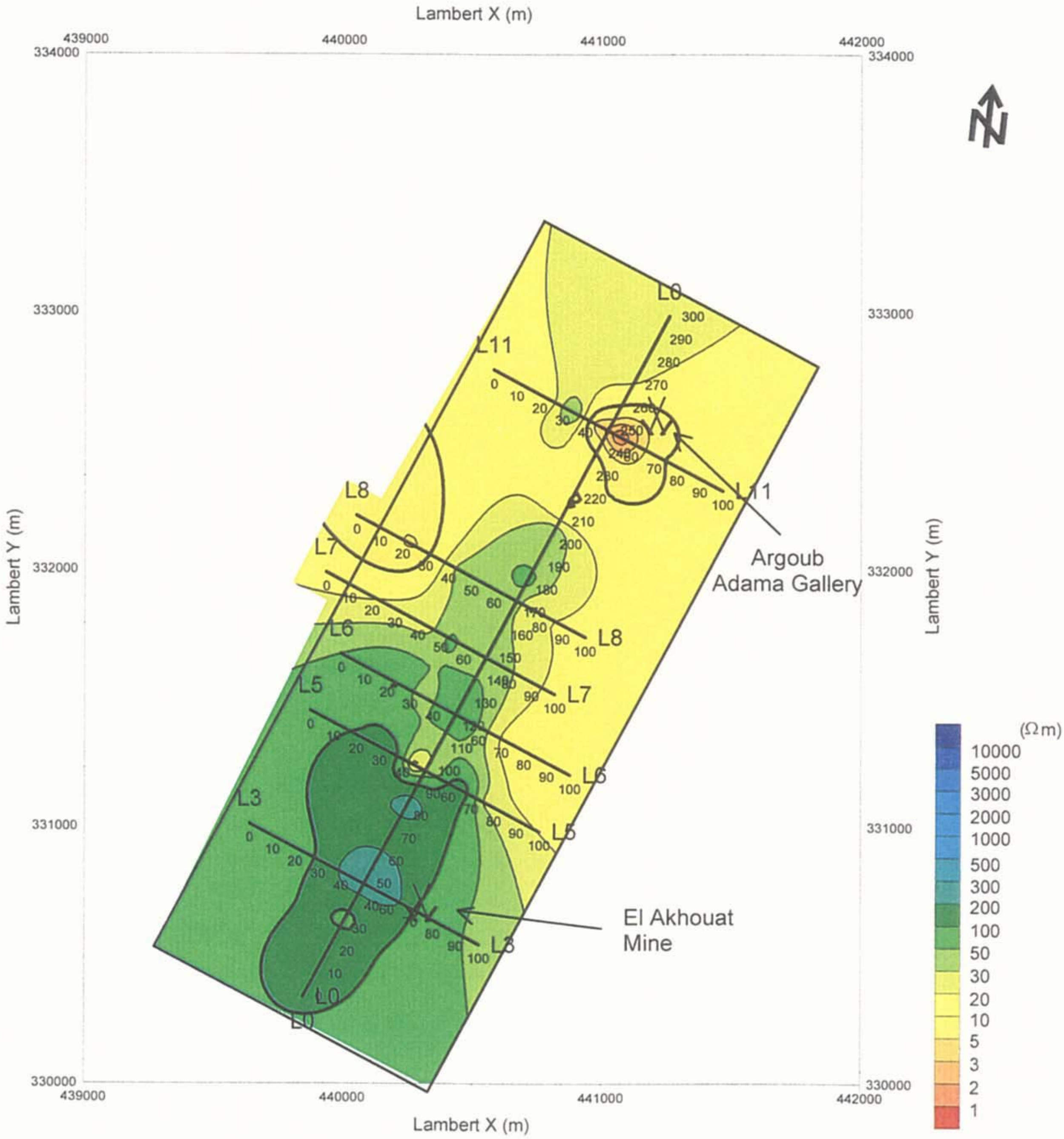

Legend

— : IP survey Line

☐ : Survey Area

X : Closed Mine

Figure 107

Plan Map of Apparent Resistivity in El Akhouat - Argoub Adama area (n=3)

Scale 1 : 25,000

March, 2000

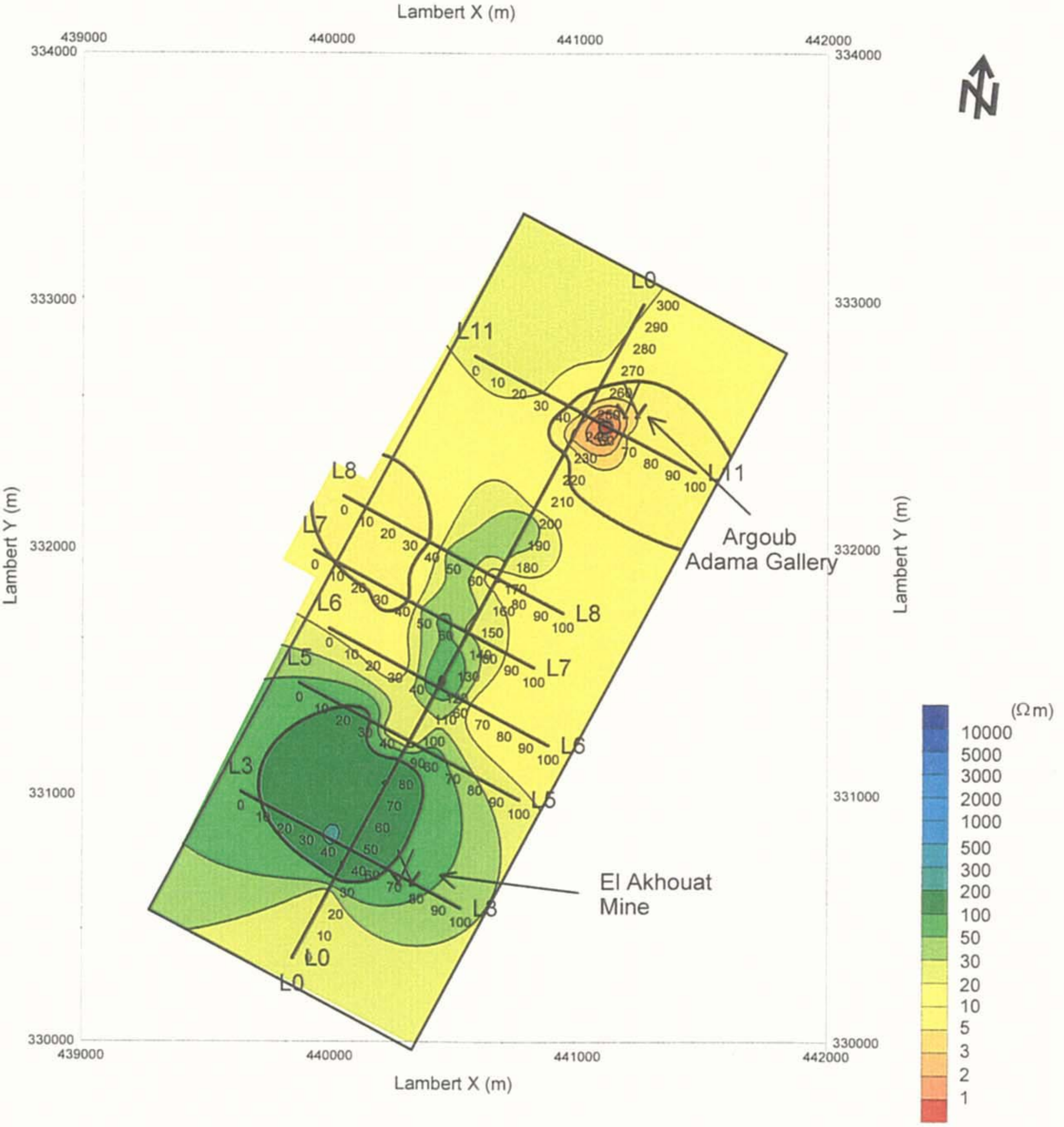

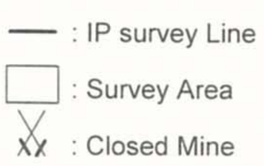

Figure 108

Plan Map of Apparent Resistivity in El Akhouat - Argoub Adama area (n=4)

Scale 1 : 25,000

March, 2000

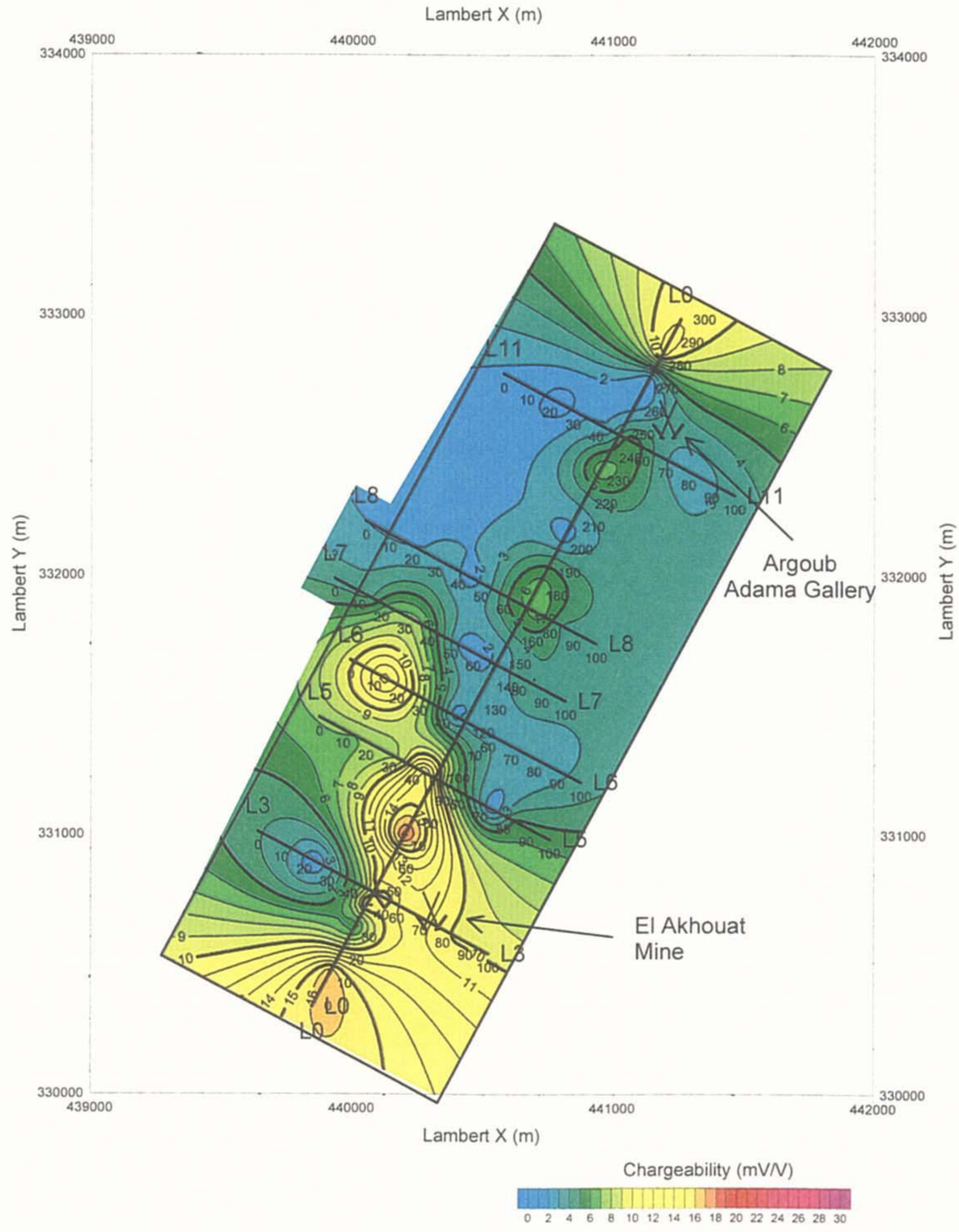

Legend

: IP survey Line

: Survey Area

: Closed Mine

Figure 109

Plan Map of Observed Chargeability in El Akhouat - Argoub Adama area (n=1)

Scale 1 : 25,000

March, 2000

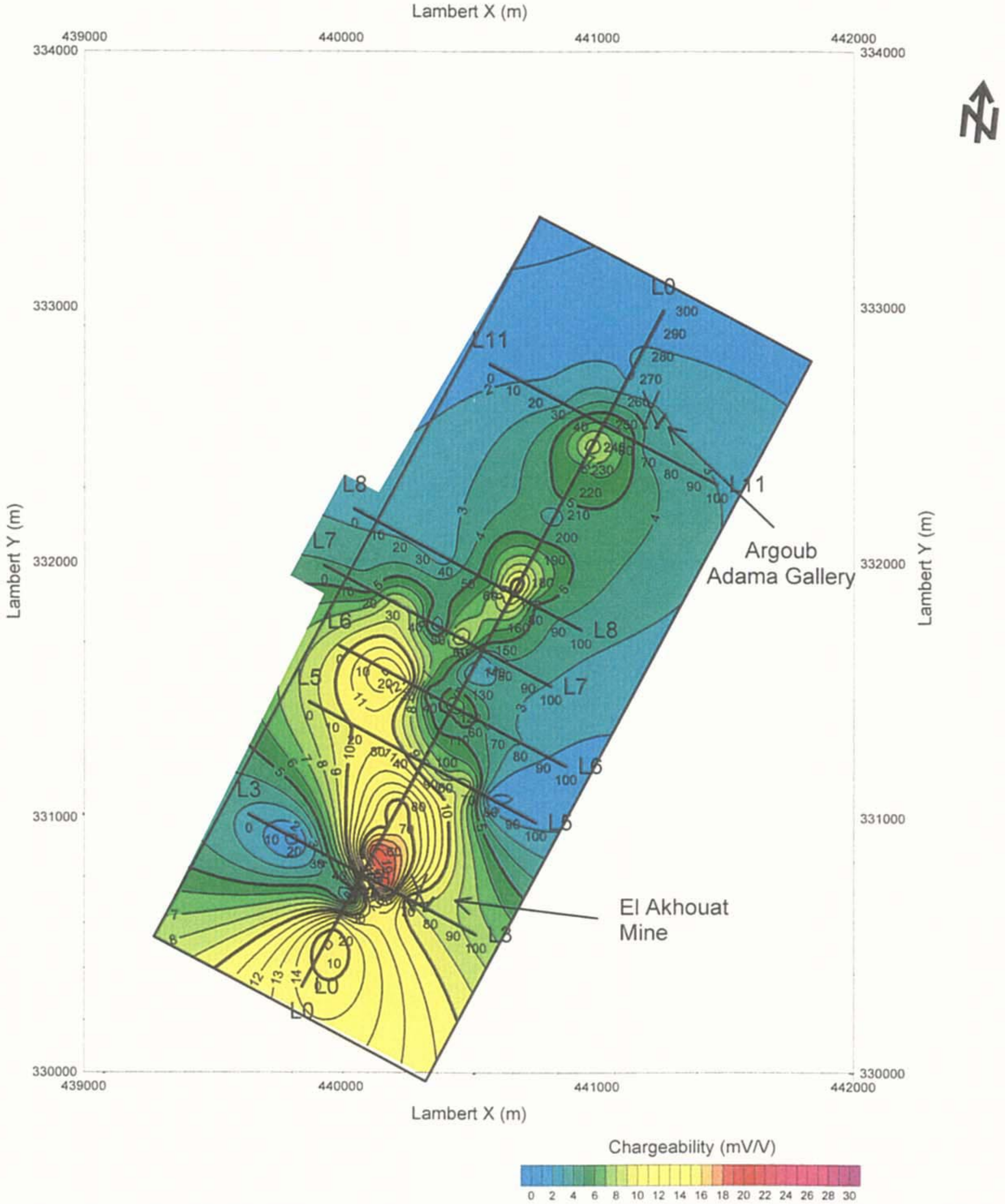

Legend

- : IP survey Line
- : Survey Area
- : Closed Mine

Figure 110

Plan Map of Observed Chargeability in El Akhouat - Argoub Adama area (n=2)

Scale 1 : 25,000

March, 2000

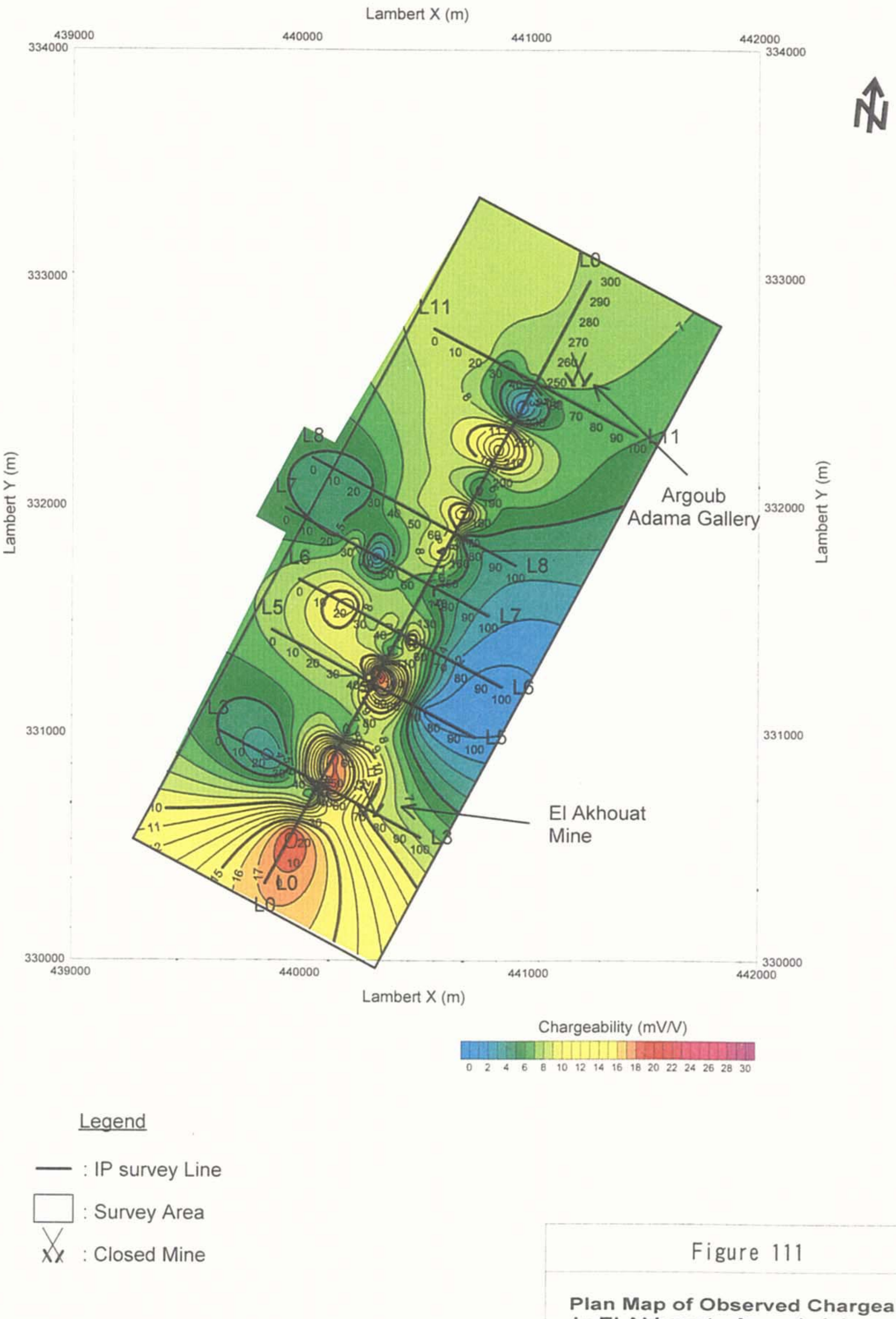

Figure 111

Plan Map of Observed Chargeability in El Akhouat - Argoub Adama area (n=3)

Scale 1 : 25,000

March, 2000

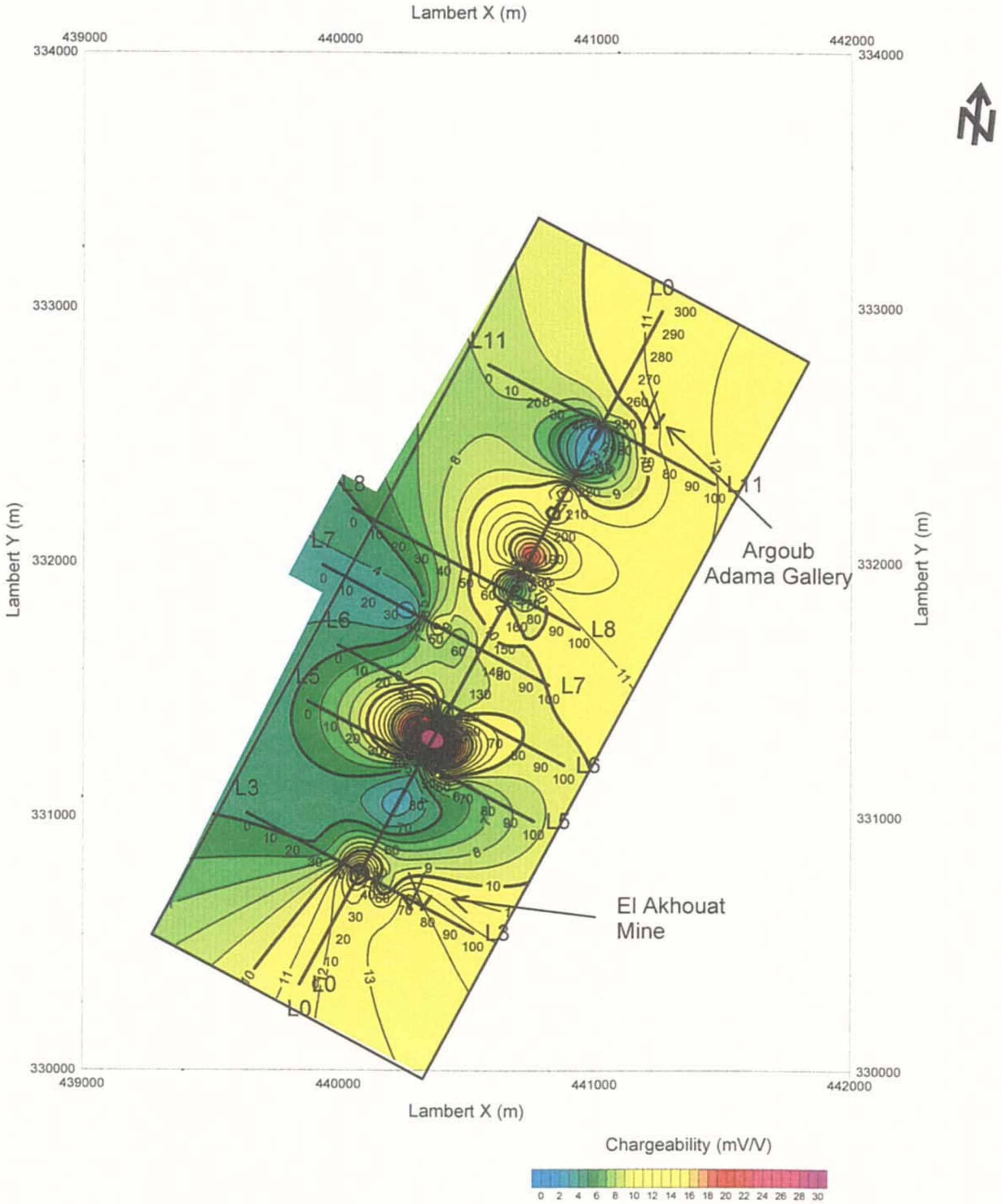

Legend

: IP survey Line

: Survey Area

: Closed Mine

Figure 112

Plan Map of Observed Chargeability in El Akhouat - Argoub Adama area (n=4)

Scale 1 : 25,000

March, 2000

classified into northern parts and another parts extending from the central parts to the southern parts. Low resistivities are widely distributed at shallow parts and become higher at lower parts in the northern survey area, where the Triassic is distributed on the ground surface. High resistivity anomaly is widely distributed at shallow parts extending from the central parts towards south, where the Cretaceous limestone lies widely. This anomaly becomes smaller with depth and the low resistivity anomaly appears at lower parts.

The resistivity distributions match with the gravity residual distributions. That is, the high and low resistivities are correlated with the high and low gravity residuals respectively. The low resistivities less than 1 Ωm, which are detected at Bou Khil prospect, are not distributed at around the station Lo-250 in the northern parts. Rocks with high resistivity generally indicate high densities, which are correlated with the Cretaceous limestone. On the other hand, rocks with low resistivity generally indicate low densities, which are correlated with the Tertiary sediment rocks. The Triassic is considered to indicate low density as shown in the gravity distributions. However, in an area where the Triassic is distributed, the Triassic indicates generally low resistivity but not extremely low resistivity and there is a case such as around the station L11-30 in the northern parts of the area, where the Triassic indicates high resistivity on the contrary.

The old mine site of El Akhouat is situated at the eastern shoulder of high resistivity anomaly and the old tunnel site of the Argoub Adama is situated at low resistivity zone. Accordingly, it is difficult to discuss directly on an indication of the resistivity related to the mineralization. Analyzed chargeabilities in the El Akhouat prospect are generally low and its maximum and approximate average values are 18 mV/V and 2.5 mV/V respectively. Negative chargeability is analyzed just on a calculation in some areas, where the useful chargeability can not be observed the same as in the Bou Khil prospect.

The old mine site of El Akhouat is situated in the vicinity of the high chargeability anomaly which is considered to be significant indicator, however the chargeability anomaly specially referred is not distributed in the vicinity of the old tunnel site of the Argoub Adama. As a results of the laboratory test, the high chargeability is not obtained at the zinc ore samples collected from the old mine site of El Akhouat. Therefore, a main factor causative of the high chargeability is not specified but a possibility is considered that the high chargeability are caused by a combination of the lead sulfides and a little chalcopyrites, which are observed in the old mine site. Considering the following that the chargeability anomalous zones extend much widely than an assumed mineralization zone and are distributed at lower parts in some places other than the known mineralization zone, the causative reason of the high chargeability should be investigated continuously in future. On the other hand, there is possibility that a ratio of the lead sulfide is low in the old tunnel site of the Argoub Adama.

The high chargeability anomalies, detected at 200 and 250 m depths around the stations L0-120 and L0-180 in the central parts of the survey area, indicate possibly sub-surface mineralization zones.

Brief characteristics on the cross sections and plans drawn from the results of data analysis are described below.

① Cross Section L0 (Figure 113)

The cross section, connecting between the old tunnel site of Argoub Adama and the old mine site of El Akhouat, runs longitudinally the survey site from the SSW to the NNE directions. The zone of high resistivity exceeding 100 Ωm is distributed at shallower parts in the southwestern side from near the station L0-210 and the zone of low resistivity less than 10 Ωm is widely distributed in lower parts. The zone of high resistivity exceeding 100 Ωm lies and continues towards the lower part, extending between the stations L0-10 and L0-100 in the south-southwestern side of the section near old mine site of the El Akhouat. High resistivity anomaly exceeding 1,000 Ωm lies in the lower part of a ridge. This high resistivity anomaly is correlated with the Cretaceous limestone.

The zone of high resistivity exceeding 100 Ωm is distributed at lower part in the north-northeastern side from near the station L0-210 and the zone of low resistivity less than 20 Ωm is distributed at shallow parts around the station L0-280 and in the north-northeastern side from the station L0-280.
The old tunnel site of the Argoub-Adama is situated in the high resistivity zone with resistivity exceeding 100 Ωm.

Judging from a condition that the low resistivity zone with resistivity less than 20 Ωm are correlated with the boundary between two resistivity structures around the station L0-210, the fault and/or crushed zone are assumed to lie in the vicinity. The fracture zones are also assumed to lie in the vicinity of the resistivity discontinuities around the stations L0-120, L0-150 and L0-280.

The high chargeability anomalies exceeding 10mV/V, distributed at shallow parts in and around the stations L0-10 and L0-100 in the southwestern section near old mine site of the El Akhouat, are nearly associated with high resistivity anomaly distributions. High chargeability anomaly exceeding 10 mV/V is distributed at 250m depth below surface and weak chargeability anomaly exceeding 10 mV/V is also distributed at 200m depth below surface around the station L0-170. These high chargeability anomalies, detected at 200m and 250m depths indicate possibly a sub-surface mineralization zone. The chargeability anomaly specially referred is not detected in the vicinity of the old tunnel site of the Argoub Adama.

② Cross Section L3 (Figure 114)

The cross section runs through the old mine site of the El Akhouat from the NW to SE directions. The zone of high resistivity anomaly exceeding 100 Ωm, which is inclining towards northwest, is widely distributed around the stations from L3-20 through -70 in the central parts of the section. This high resistivity anomaly is correlated with the Cretaceous limestone.

The low resistivity structure with 50 Ωm is rising up from the lower part around the station L3-60 and dividing the high resistivity anomaly at shallow parts. This is associated with the rising structure of gravity basement described previously and considered to correlate with the Triassic. The old mine site of the El Akhouat is situated in and around the rising structure of resistivity. The low resistivity anomaly less than 10 Ωm, extends from the station L3-90 to the southeastern parts, are considered to correlate with the Tertiary sedimentary rocks distributed in the open field.

The high chargeability anomaly exceeding 10 mV/V is distributed extending from the stations L3-30 to L3-80 in the central parts of the section. The strong anomaly of the chargeability exceeding 20 mV/V around the station L3-60 is distributed in the central parts of the anomaly, indicating a triangular shape centered the rising pattern of narrow low resistivity zone. The old mine site of the El Akhouat is located in and around the high chargeability anomaly.

③ Cross Section L5 (Figure 115)

The cross section runs through north-northeast side parallel to the line L3 with 500m spacing. The high resistivity anomaly exceeding 100 Ωm, which is widely distributed at shallow parts in and around the stations L5-0 through -80 in the central section, is correlated with the Cretaceous limestone.

The low resistivity anomaly less than 10 Ωm, which is correlated with the Triassic around the station L0-100 in the central parts of the section, extends from the lower parts to the shallower parts dividing the high resistivity anomaly to two anomalies. That vicinity corresponds to thick parts of the surface layer with high density on the cross sectional gravity analysis and the low resistivity anomaly mentioned above is considered to be as narrow as it does not appear on cross sectional gravity analysis. The low resistivity anomaly less than 10 Ωm in the southeastern parts of the section is considered to correlate with the Tertiary sedimentary rocks, which are distributed in an open field, extends from the lower parts to the shallower parts.

The high chargeability anomaly exceeding 10 mV/V is widely distributed at the upper section of low resistivity anomaly extending from the lower parts to the shallower parts.

④ Cross Section L6 (Figure 116)

The cross section, which is situated at the central parts of the survey area, runs through north-northeast side parallel to the line L5 with 250m spacing. The small anomaly of high resistivity exceeding 100 Ωm is distributed in and around the stations L6-30 and L6-60 in the central parts of the section and the resistivity tends to become lower with depth at its lower parts. The low resistivity anomalies less than 10 Ωm are distributed in both ends of the section. They are considered to correlate with both the Tertiary sediment rocks in southeastern end and the Triassic in northwestern end respectively.

The high chargeability anomaly exceeding 10 mV/V is distributed extending from the northwestern end to the lower parts in the central section and it become higher with depth. This characteristics of the chargeability anomaly matches with the feature that the anomaly is recognized at 250m below surface around the station L0-120 of the line L0.

⑤ Cross Section L7 (Figure 117)

The cross section runs through north-northeast side parallel to the line L6 with 250m spacing. The resistivity of the section is generally lower than that for previous three sections and small high anomaly exceeding 100 Ωm is only recognized around the station L7-30. The low resistivity anomaly less than 10 Ωm distributed in the lower parts of high anomaly is considered to correlate with the Triassic. The low zone with resistivity less than 20 Ωm, which is distributed in the lower parts extending from the L0-150 to southeastern side, matches with an inferred jut structure of gravity basement with low density.

The chargeability anomaly specially referred is not recognized and it corresponds to the feature that the significant chargeability anomaly is not detected around the station L0-150 in the line L0.

⑥ Cross Section L8 (Figure 118)

The cross section runs through north-northeast side parallel to the line L7 with 250m spacing. The low resistivities less than 20 Ωm are entirely distributed on the section and it tends to become higher at shallow parts around the central section and become lower at both ends of the section.

The low resistivity anomalies less than 10 Ωm, which are distributed extending from the stations L8-0 to -20 in the northwestern end and also extending from the stations L8-80 to -100 in the southeastern end of the section, are considered to correlate with the Triassic and the Tertiary sedimentary rocks respectively.

The chargeability anomaly exceeding 10 mV/V with a triangular shape is distributed extending from the lower parts to the shallow parts around central section. This characteristic pattern on the chargeability distributions correspond to the feature that the chargeability anomaly is detected at 200m depth below surface around the station L0-180 in the line L0. In case this chargeability anomaly is assumed to be an indication of mineralization, the zone of low resistivity less than 30 Ωm is possibly correlated with the Triassic.

⑦ Cross Section L11 (Figure 119)

The cross section runs near the old tunnel site of the Argoub Adama through north-northeastern parts of the survey site from the NW to the SE directions. The zone of low resistivity less than 10 Ωm is widely distributed extending from around the stations L11-30 to L11-80 in the central parts of the section. Especially, strong anomaly with low resistivity less than 1 Ωm is distributed around the station L11-40. The high resistivity anomaly exceeding 100 Ωm, which is distributed extending from the stations L11-10 to L11-20 in the northwestern parts of the section, and forms a discontinuity contrasted with low resistivity zone around station L11-30.

Significant chargeability anomaly is not detected other than the weak anomaly exceeding 5 mV/V around station L11-60 near old tunnel site of the Argoub Adama.

⑧ Resistivity Distribution Plan: 200m above sea level (Figure 120)

The resistivity tends generally to be high in the southwestern and northern parts, and to be low in the western and southeastern parts of the survey area. High resistivity anomalies exceeding 100 Ωm are distributed in and around the stations L3-10 to L3-40 in the southwestern parts and the station L5-70 in the southern parts of the survey area. Low resistivity anomalies less than 10 Ωm with the direction of NNW-SSE, which extend from near the station L8-0 to L5-40, are distributed in line dividing those high resistivity anomalies. A constricted pattern of relatively low resistivity anomaly is indicated in and around of the old mine site of the El Akhouat where is corresponding to an extension of low resistivity anomalies line with NNE-SSW direction. The low resistivity anomaly, which is widely distributed in the southeastern parts of the survey area, are correlated with the Triassic or Tertiary sedimentary rocks. The low resistivity anomaly is also distributed in the southern side of the Argoub-Adama old tunnel site, which is situated around resistivity discontinuity with NW-SE direction. Those features are corresponding to an indication obtained from

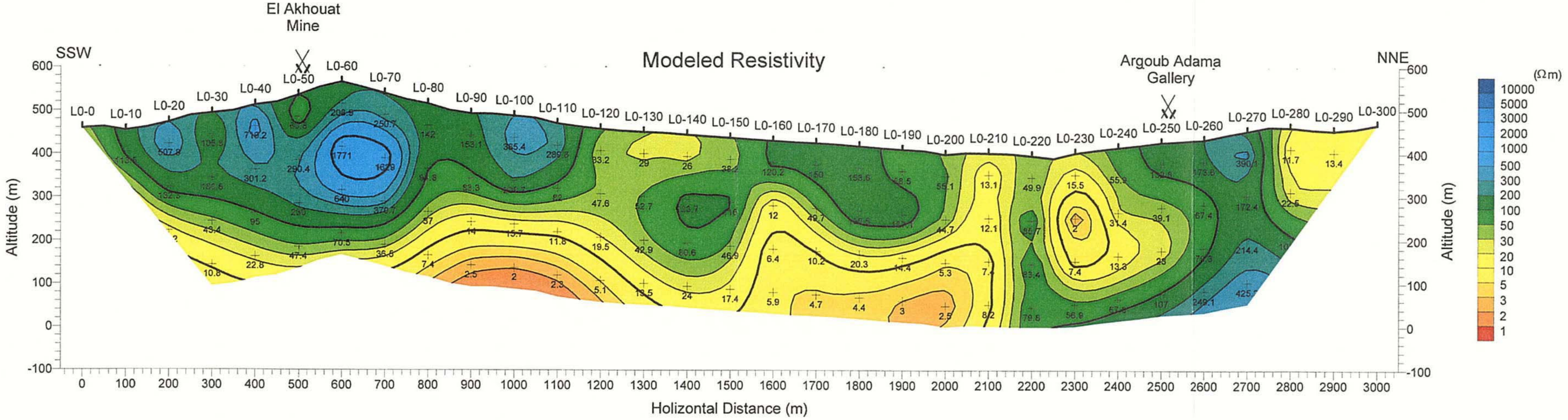

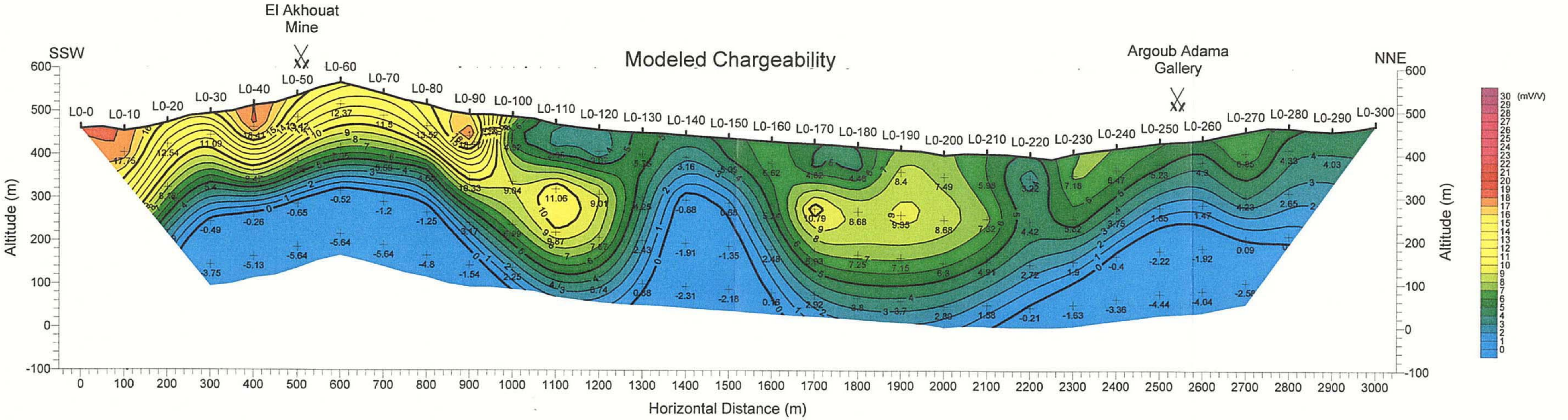

Figure 113 Modeled IP cross-section (Line L0)

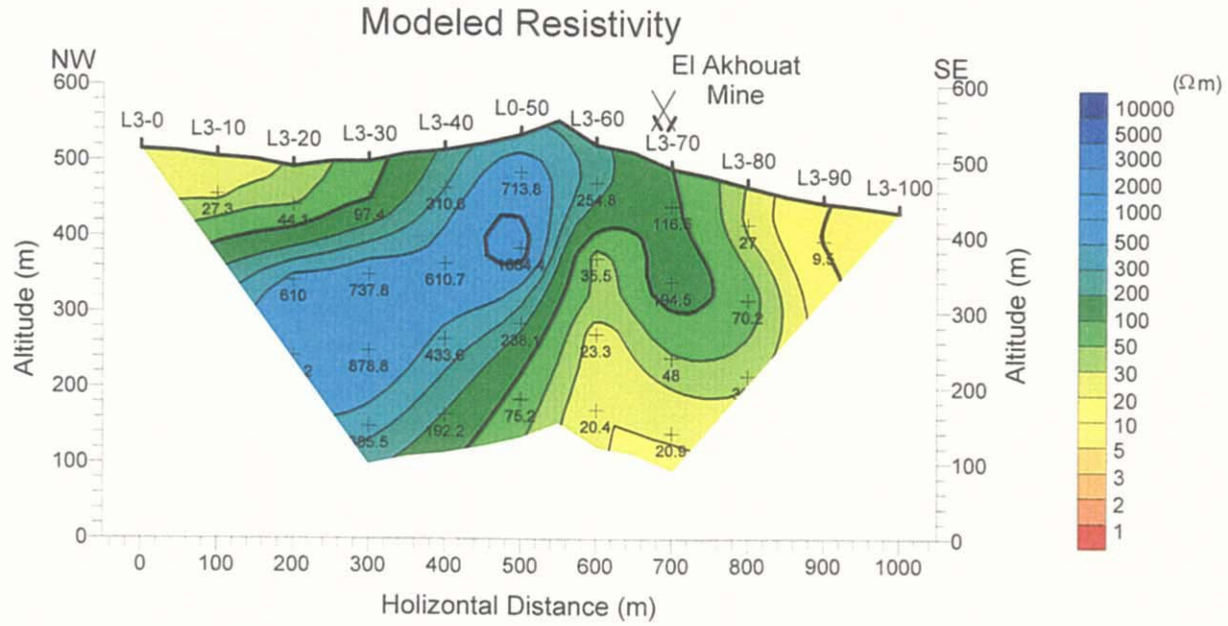

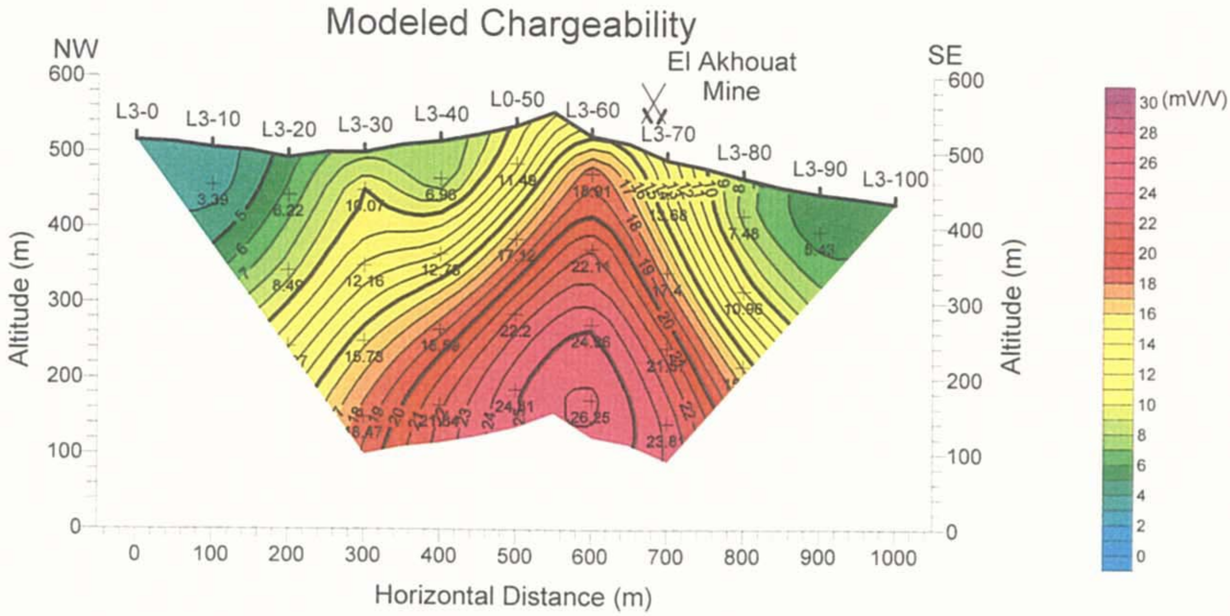

Figure 114 Modeled IP cross-section (Line L3)

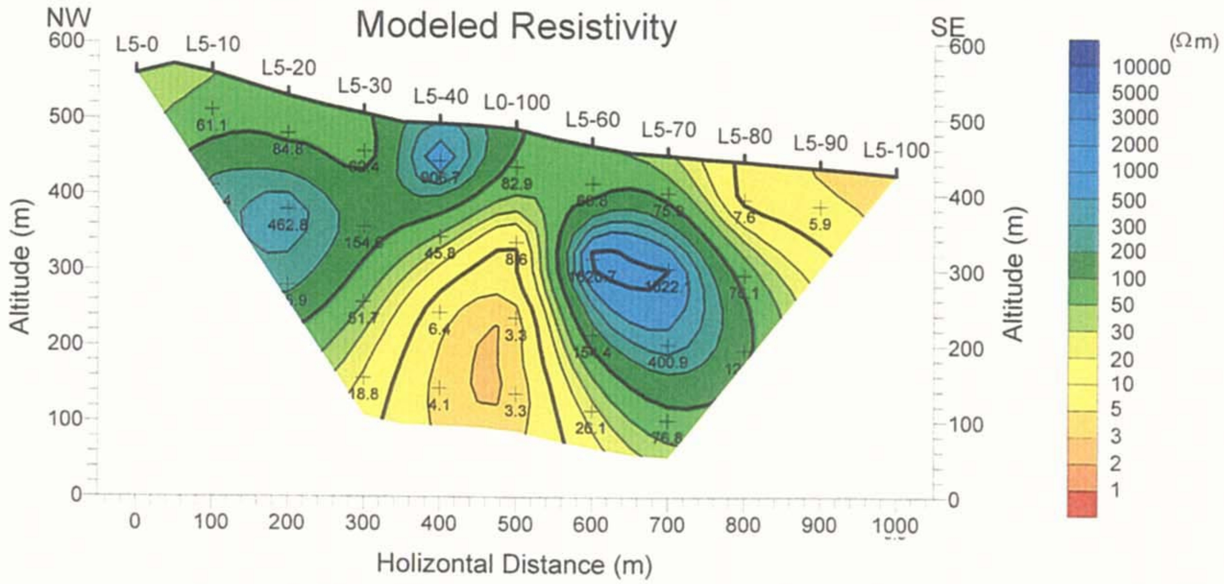

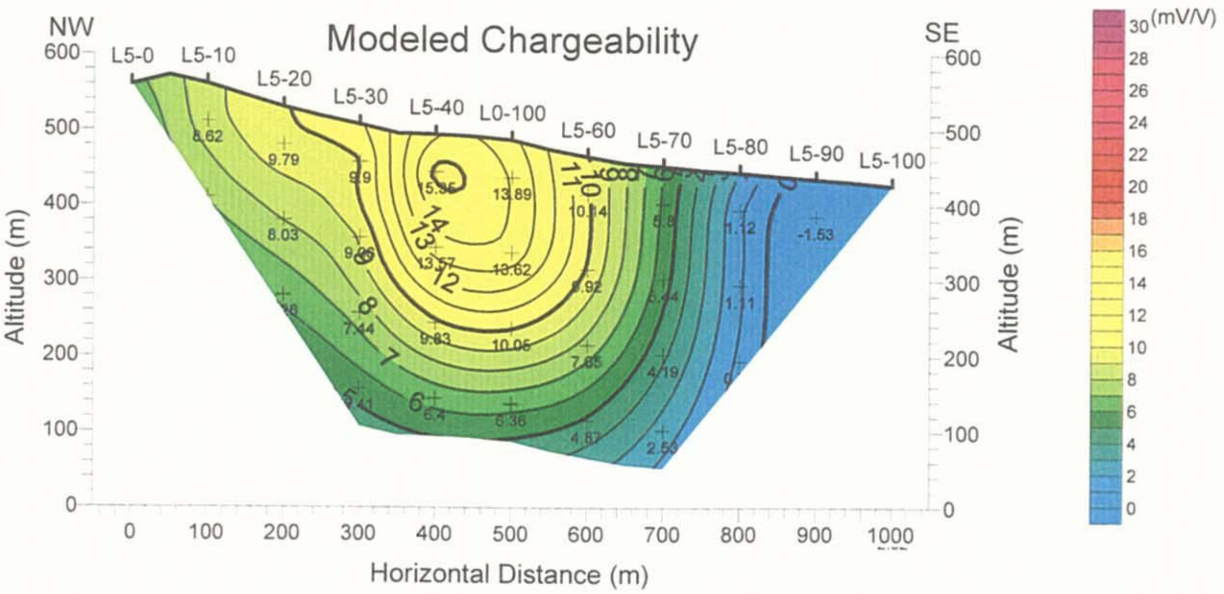

Figure 115 Modeled IP cross-section (Line L5)

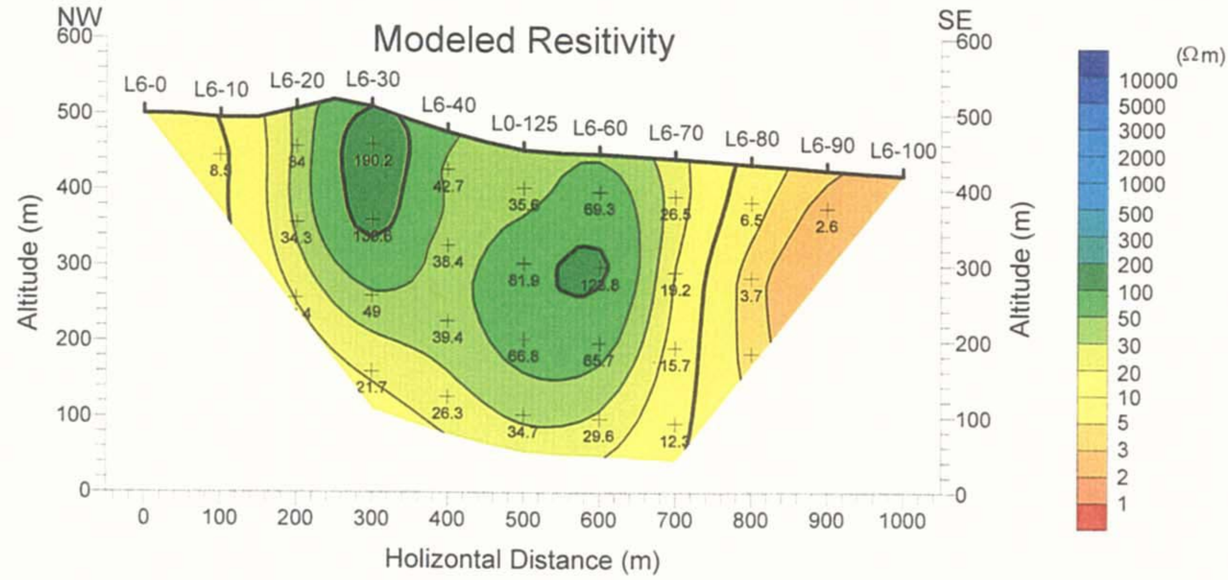

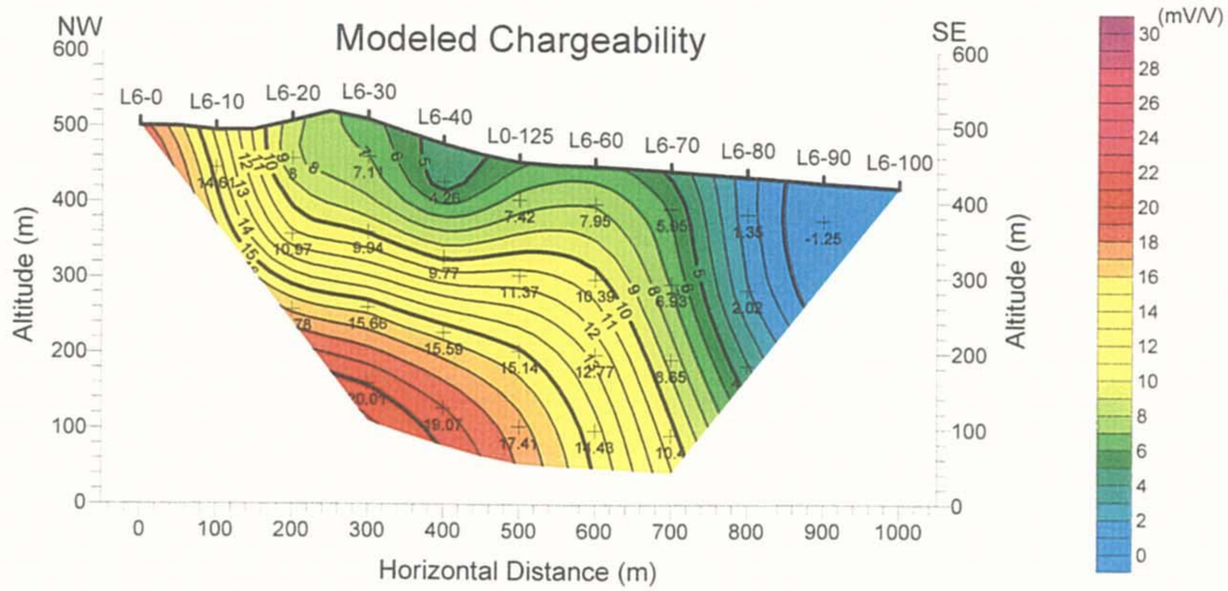

Figure 116 Modeled IP cross-section (Line L6)

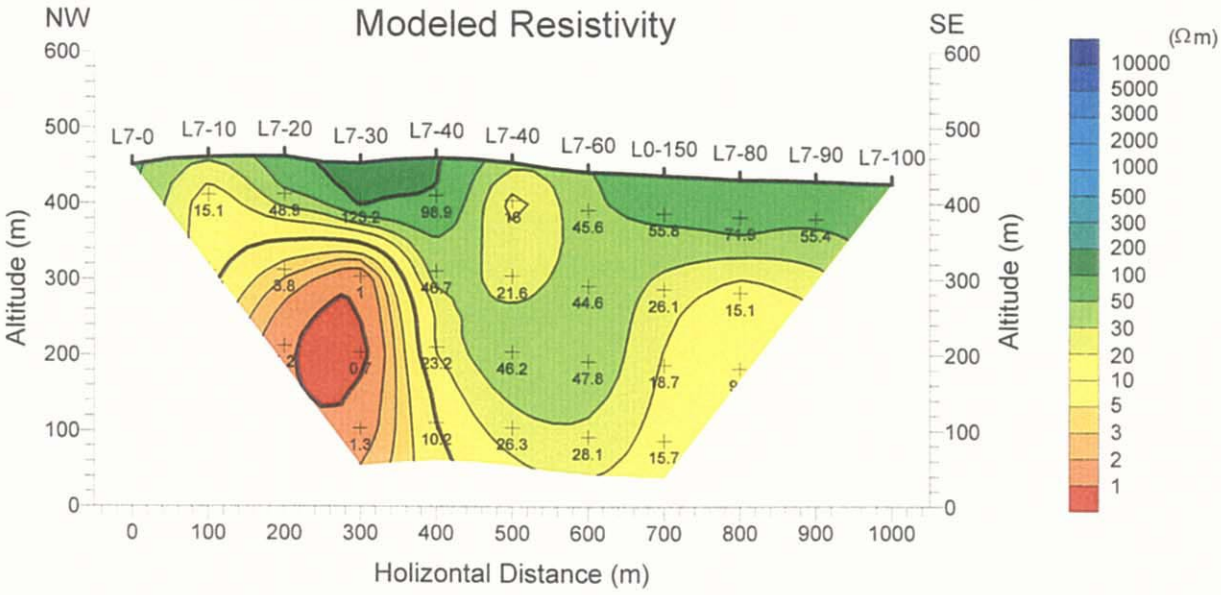

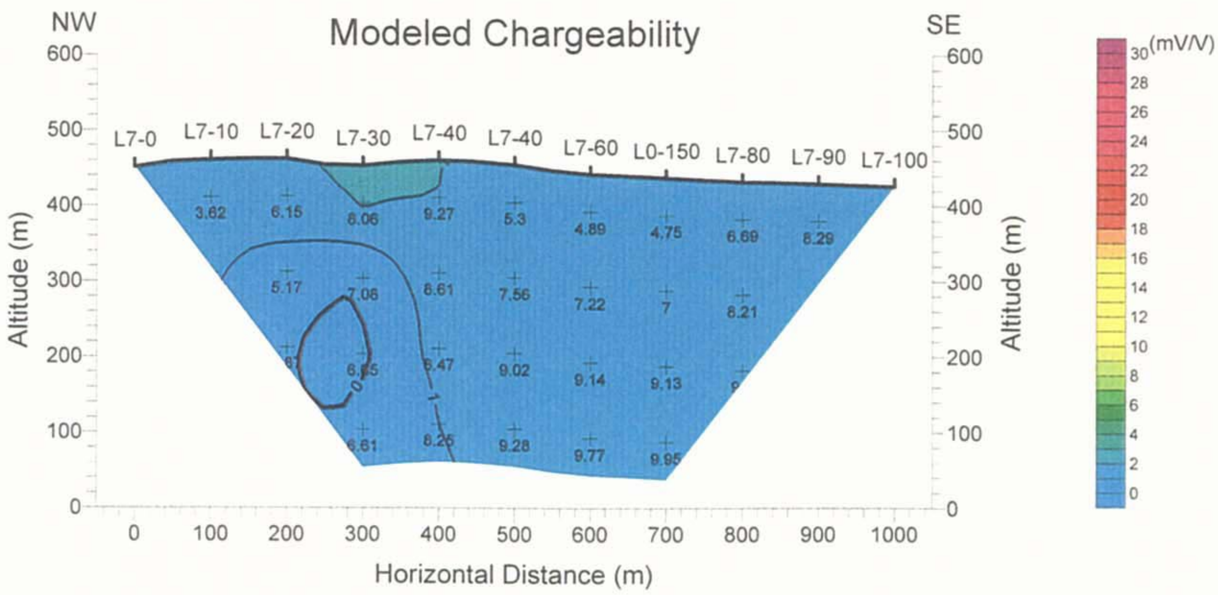

Figure 117 Modeled IP cross-section (Line L7)

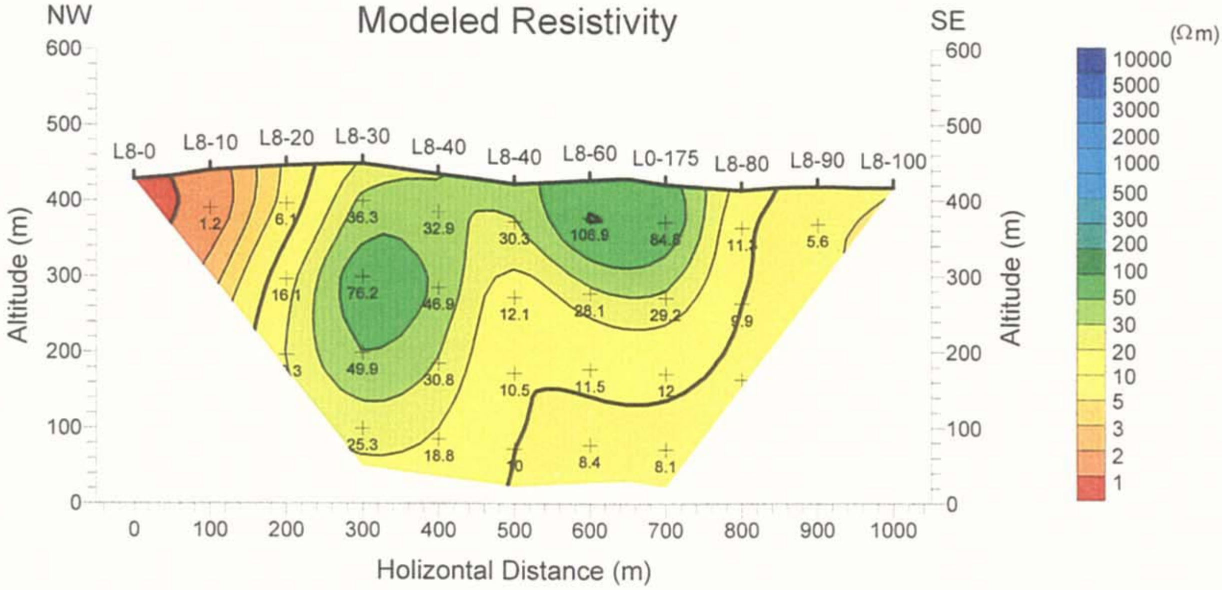

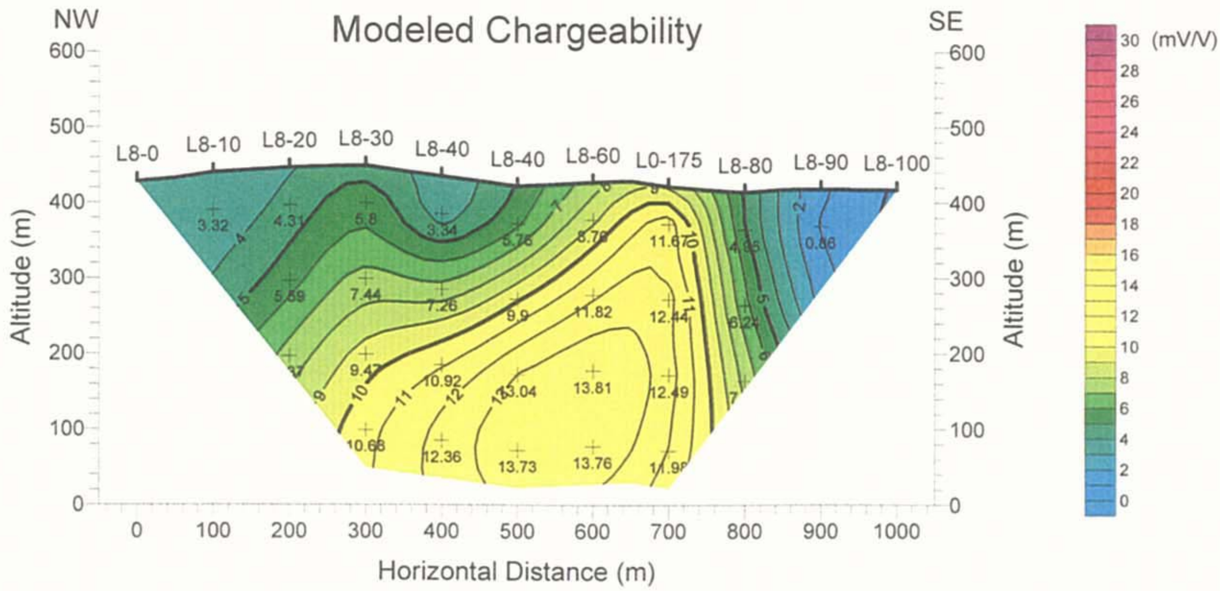

Figure 118 Modeled IP cross-section (Line L8)

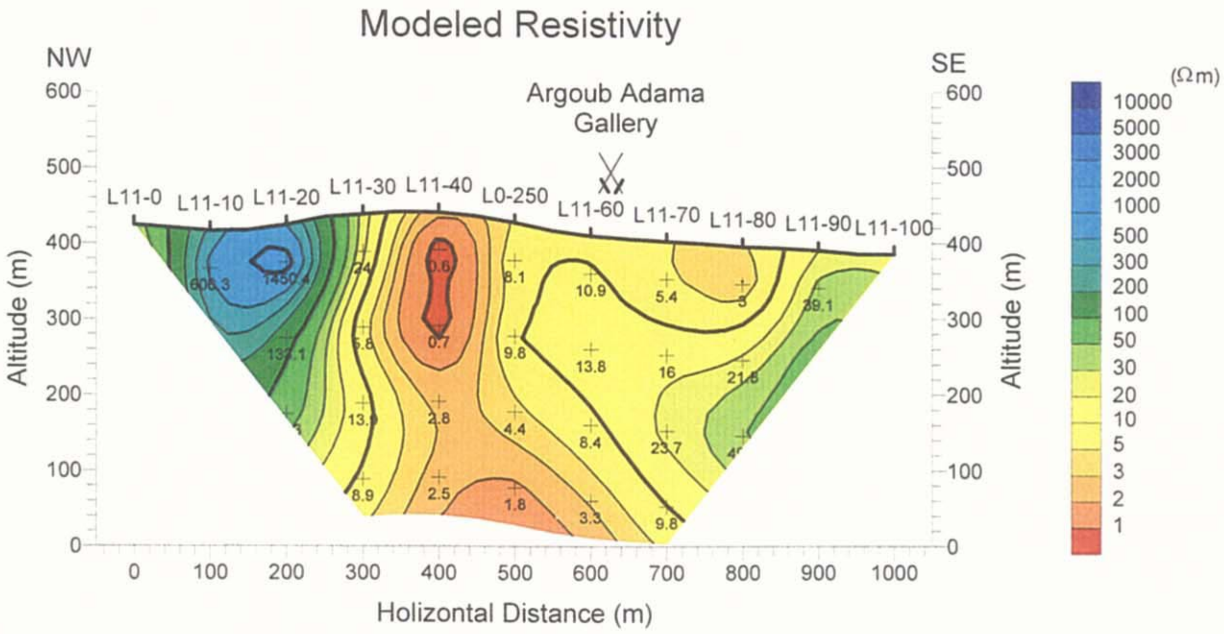

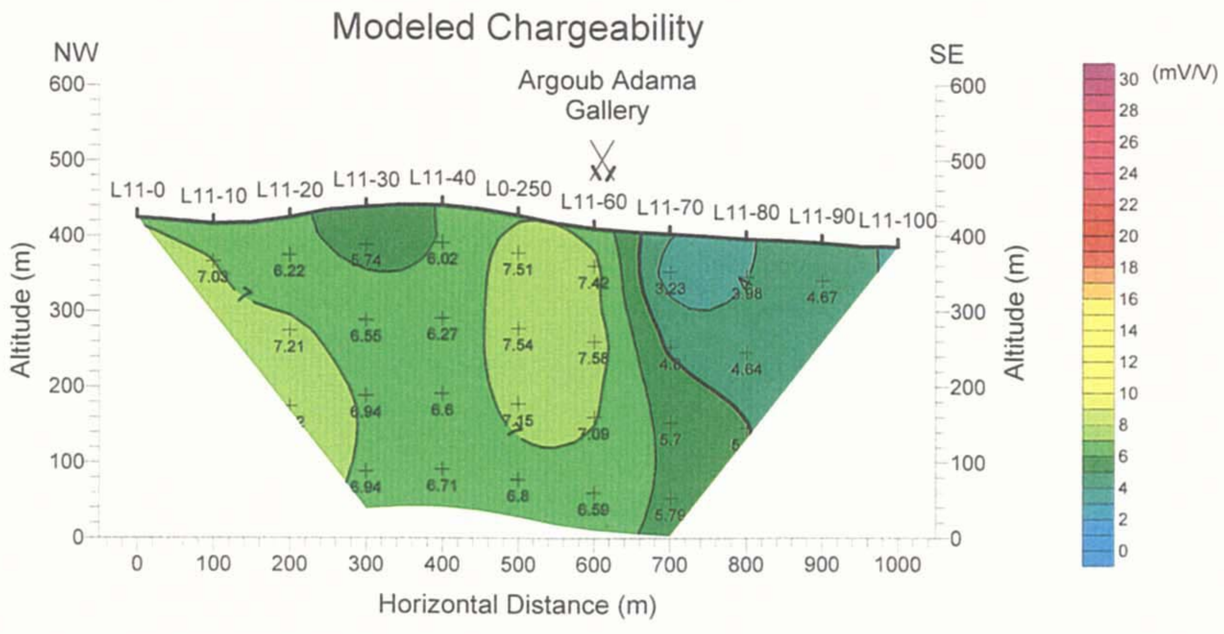

Figure 119 Modeled IP cross-section (Line L11)

the interpretation of the gravity first vertical derivative.

⑨ Resistivity Distribution Plan:300m above sea level (Figure 121)

The resistivity distributions are similar as previous plan, however the resistivities become entirely higher. Two high resistivity anomalies exceeding 100 Ωm, which are distributed extending from the station L3-10 to L3-40 and around station L5-70 in the southern parts, are combined into single anomaly. Small high resistivity anomalies exceeding 100 Ωm are also distributed around station L0-180 in the central parts and L11-20 in the northern parts.

⑩ Resistivity Distribution Plan:400m above sea level (Figure 122)

The resistivities indicate generally the similar pattern with previous plans. However the resistivity become entirely higher and the distribution zone of low resistivities becomes narrower. The high resistivity zone is distributed in the northwestern side of the line L0. The high resistivity anomaly, which is correlated with the Cretaceous limestone in the southern parts of the survey area, exceeding 100 Ωm extends to the east and west directions. Such features are corresponding to the residual gravity anomaly described previously.

⑪ Chargeability Distribution Plan:200m above sea level (Figure 123)

High chargeability anomaly exceeding 10 mV/V is distributed extending from the central parts to the southern parts of the survey area. The strong chargeability anomaly with a maximum value exceeding 20 mV/V is distributed extending from the stations L3-20 to L3-80 and the old mine site of the El Akhouat is located within that anomaly zone.

Strong chargeability anomaly with a maximum exceeding 20 mV/V is also distributed extending from the stations L6-0 to L6-40 in the western parts and the high anomaly exceeding 10 mV/V is distributed extending from the stations L8-40 to L0-175 in the central parts of the survey area. However an indication on the mineralization related to those anomalies is not recognized on the ground. The chargeability anomaly specially referred is not detected in the vicinity of the old tunnel site of the Argoub Adama, where the weak chargeability anomaly exceeding 5 mV/V is only recognized.

⑫ Chargeability Distribution Plan:300m above sea level (Figure 124)

The chargeability distributions indicate the similar pattern with previous plan. High chargeability anomalies exceeding 10mV/V are distributed in the vicinity of the old mine site of the El Akhouat. High chargeability anomalies exceeding 10mV/V are also distributed around the station L0-0 in the southern end and around the stations extending from L6-0 to L0-40 in the western parts. The latter is extending to the vicinity of the station L5-60 in the southeastern parts. High chargeability anomalies exceeding 10mV/V, which are recognized widely in the central parts on previous plan for elevation at 200m, changes to small anomaly around station L8-40.

The chargeability anomaly specially referred is not detected in the vicinity of the old tunnel site of the Argoub Adama, where the weak chargeability anomaly exceeding 5 mV/V is only recognized.

⑬ Chargeability Distribution Plan:400m above sea level (Figure 125)

The chargeability distributions are similar with previous plan for elevation at 300m other than that the high chargeability anomaly exceeding 10mV/V is not recognized around the station L8-40. High chargeability anomalies exceeding 10mV/V are also distributed around the station L0-0, around the stations extending from L5-30 to L5-60 and extending widely from near the station L3-70 in the vicinity of the El Akhouat old mine site to the southern parts.

(3) Considerations and Summaries

Relations between the results obtained from the IP survey and the known ore deposits is summarized and shown in Figure 126. The old mine site of El Akhouat and the old tunnel site of the Argoub Adama, which are known as the ore deposits or indications related to the mineralization in the survey area, are located respectively in the southern and northern parts of the survey area. Both are situated at the contact zone between the Cretaceous and Triassic systems. The Triassic is widely distributed in the northern parts and the Cretaceous in the southeastern parts is widely covered by the Quaternary. Conversely the Cretaceous limestone is widely distributed in the southern parts and the Triassic in the northern parts extends long and slenderly towards the old mine site of El Akhouat.

The Cretaceous limestone is grasped as the high resistivity layer with high density. The high resistivity layer distributed thick at shallow parts is considered to correlate with such Cretaceous limestone. The low resistivity anomalies extend from the lower parts towards the high resistivity layer at shallow parts in the line L3, running through the old mine site of El Akhouat and the lines L5, L6, L8. Those are considered to correlate the Triassic. This low resistivity anomaly is corresponding to the rising up structure of the gravity basement with low density and the chargeability anomalies are distributed around the vicinity of the rising structure. The chargeability anomalies appear from the shallow parts in the lines L0, L3, L5 and L6 but the chargeability anomalies are distributed at lower parts around the point, where line L0 intersect the line L8 in the central parts of the survey area. The latter, also detected by the IP survey adopted the three electrode array which are carried out by ONM , is possible to be an indication of sub-surface mineralization.

The lower and shallow parts indicate respectively the low and high

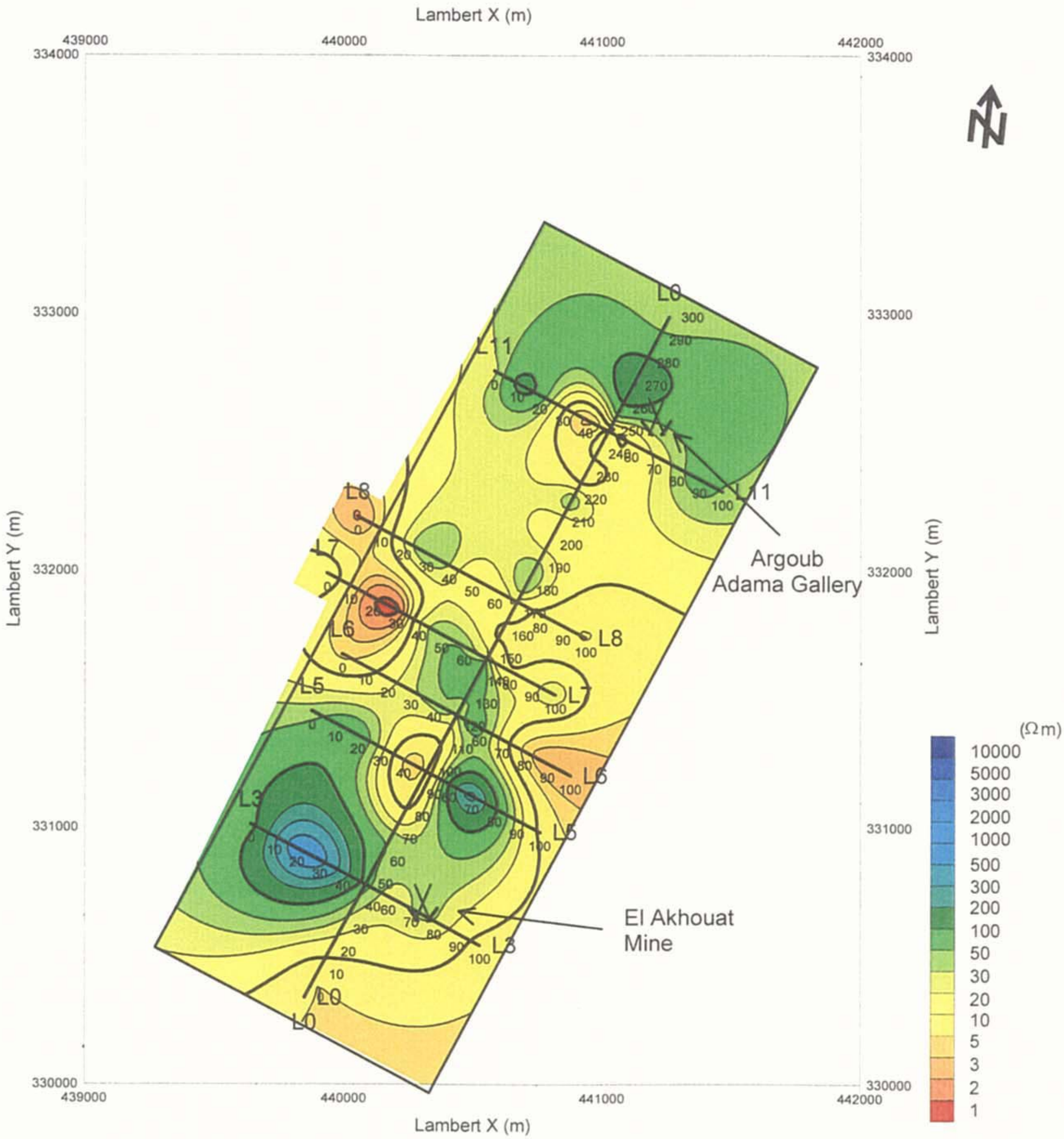

Legend

: IP survey Line

: Survey Area

: Closed Mine

Figure 120

Plan Map of Modeled Resistivity in El Akhouat - Argoub Adama area (Altitude: 200m)

Scale 1 : 25,000

March, 2000

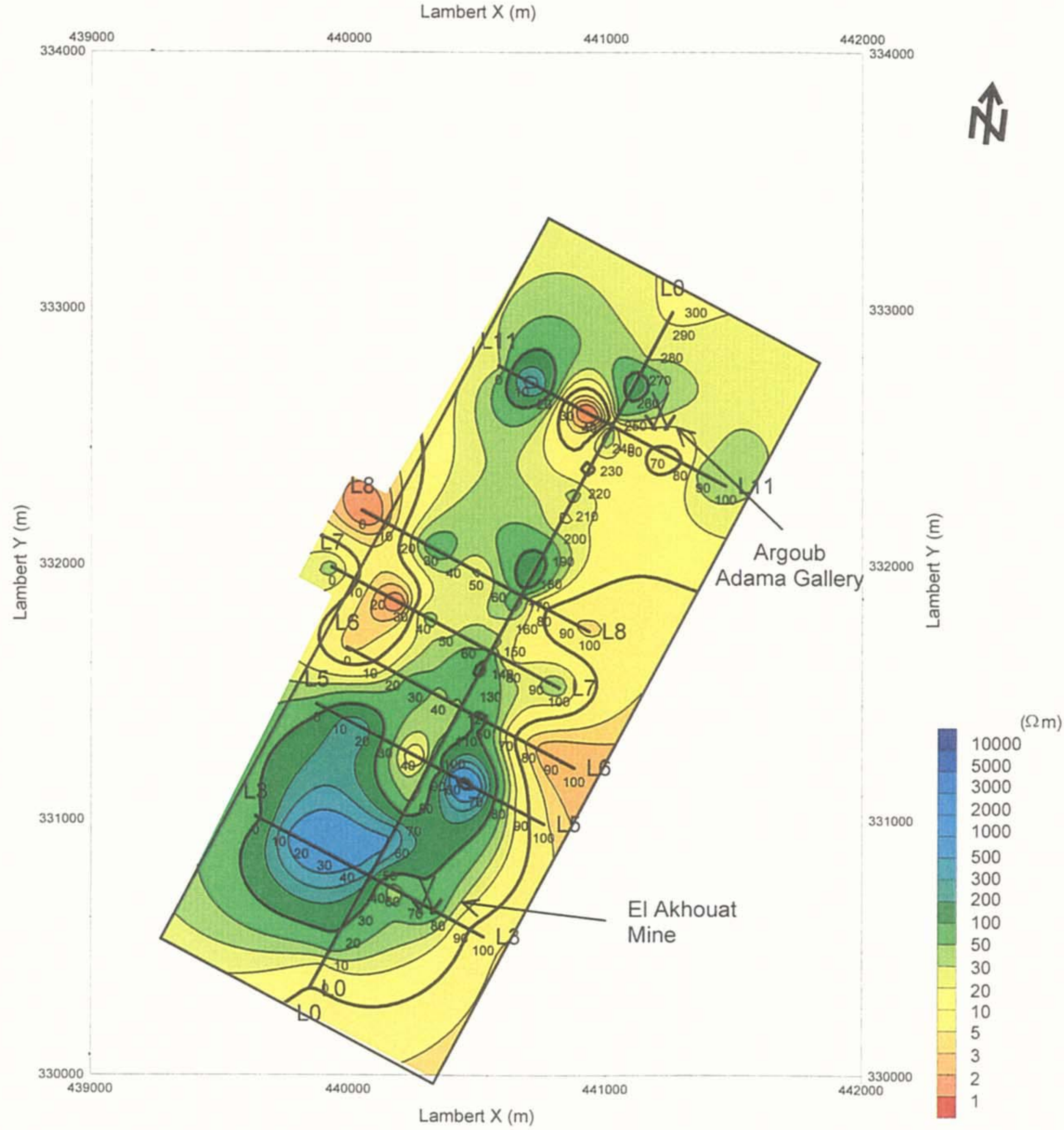

Legend

— : IP survey Line

☐ : Survey Area

XX : Closed Mine

Figure 121

Plan Map of Modeled Resistivity in El Akhouat - Argoub Adama area (Altitude: 300m)

Scale 1 : 25,000

March, 2000

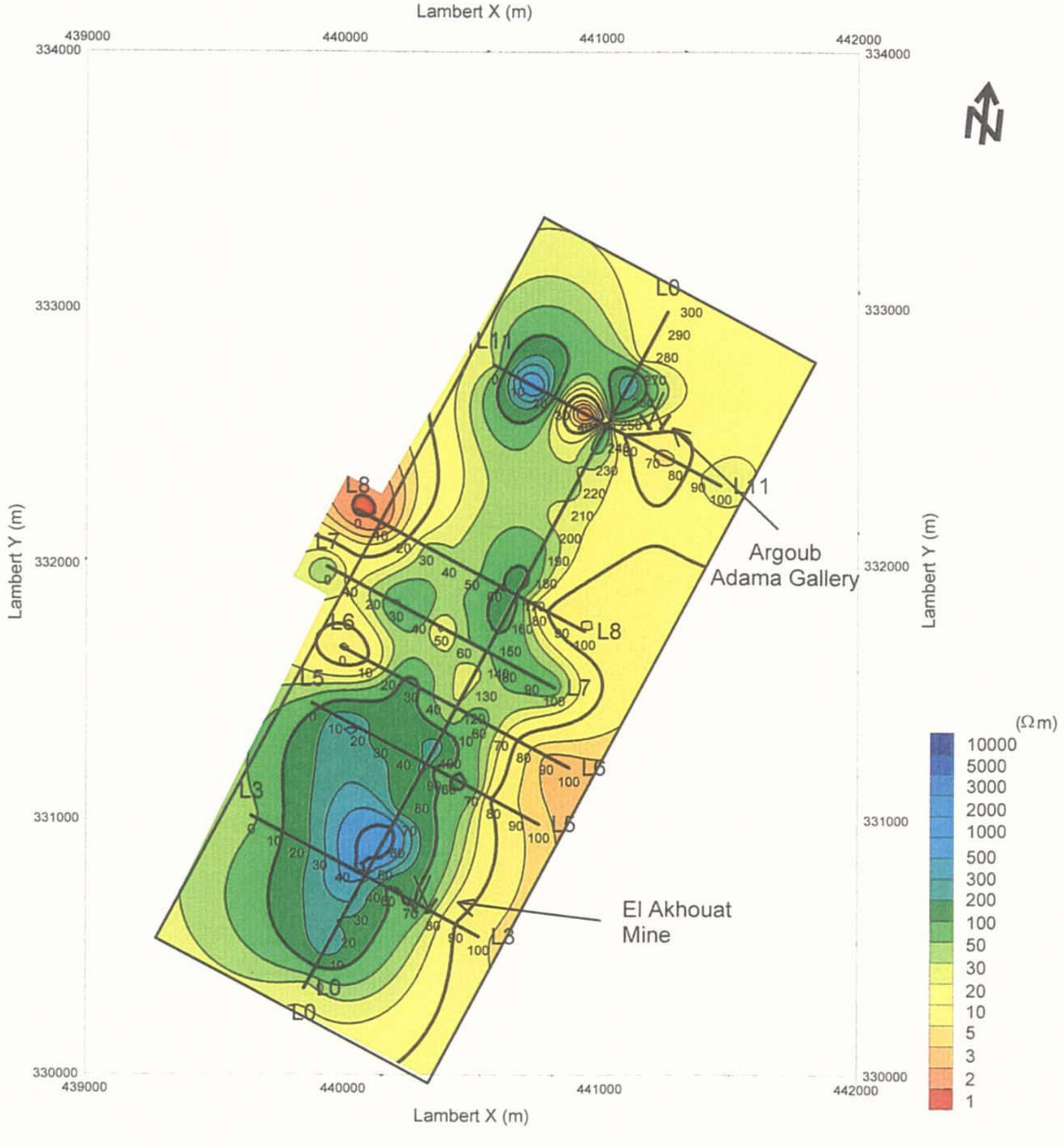

Legend

- : IP survey Line
- : Survey Area
- : Closed Mine

Figure 122

Plan Map of Modeled Resistivity in El Akhouat - Argoub Adama area (Altitude: 400m)

Scale 1 : 25,000

March, 2000

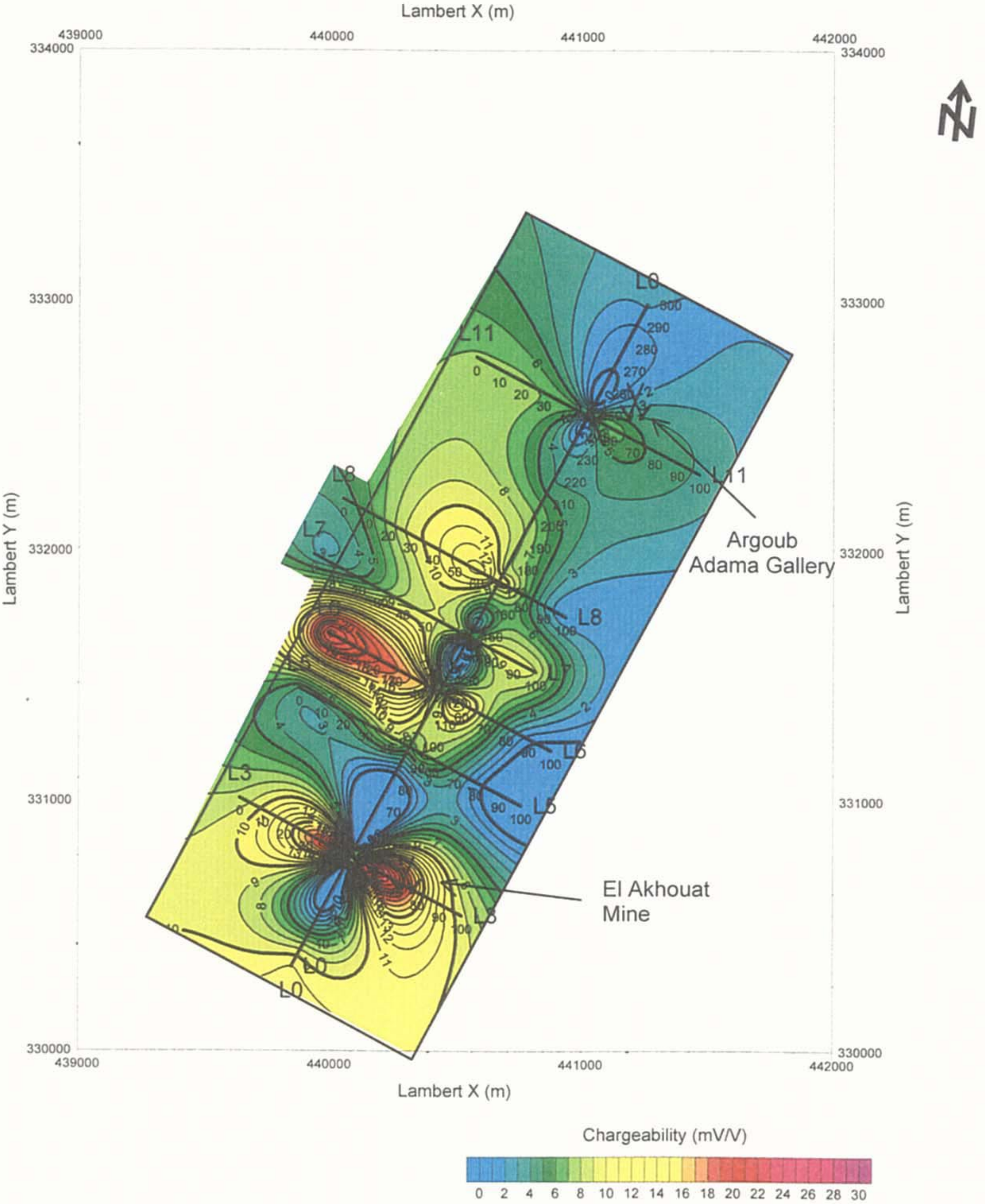

<u>Legend</u>

— : IP survey Line

☐ : Survey Area

XX : Closed Mine

Figure 123

Plan Map of Modeled Chargeability in El Akhouat - Argoub Adama area (Altitude: 200m)

Scale 1 : 25,000

March, 2000

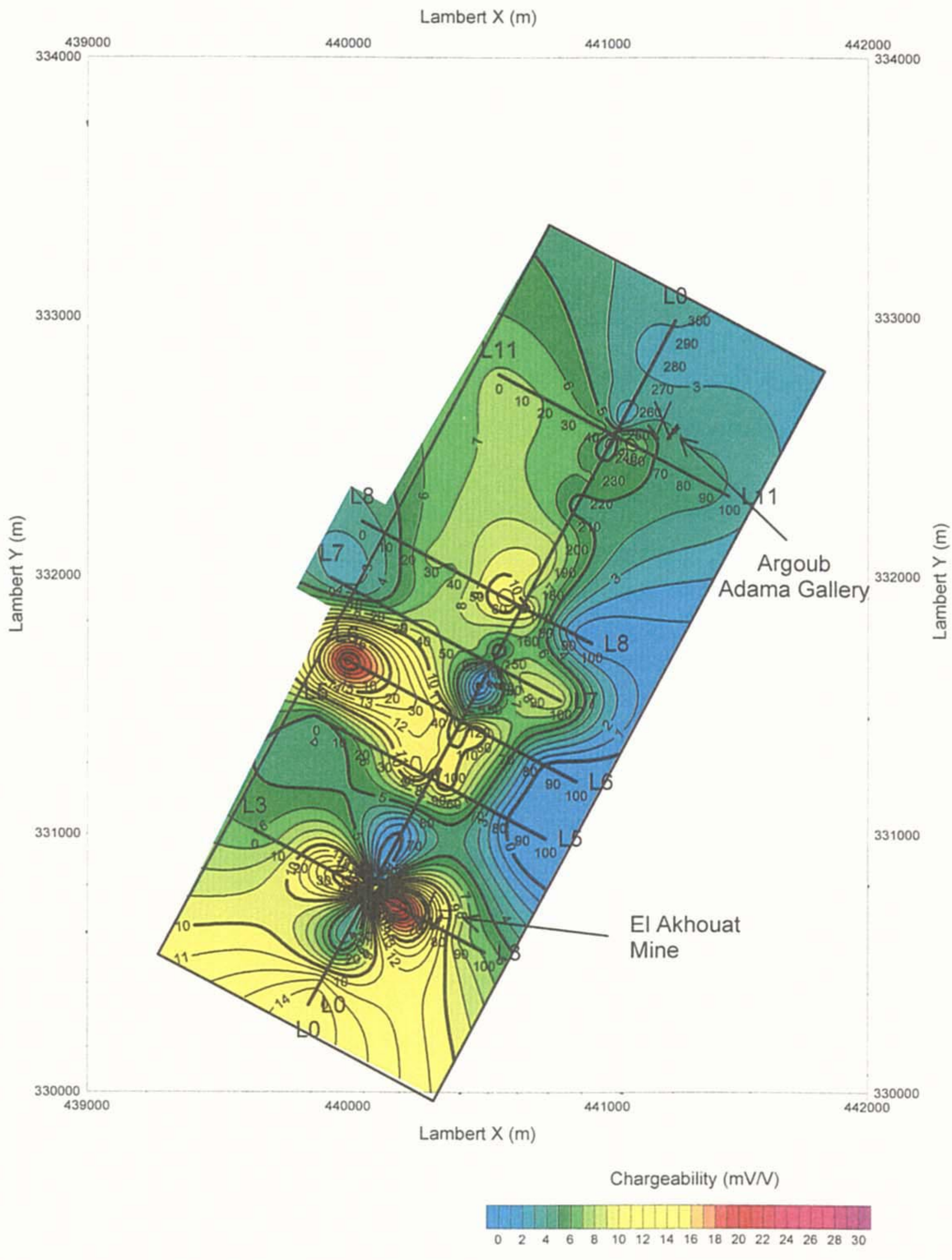

Legend

— : IP survey Line

: Survey Area

: Closed Mine

Figure 124

Plan Map of Modeled Chargeability in El Akhouat - Argoub Adama area (Altitude: 300m)

Scale 1 : 25,000

March, 2000

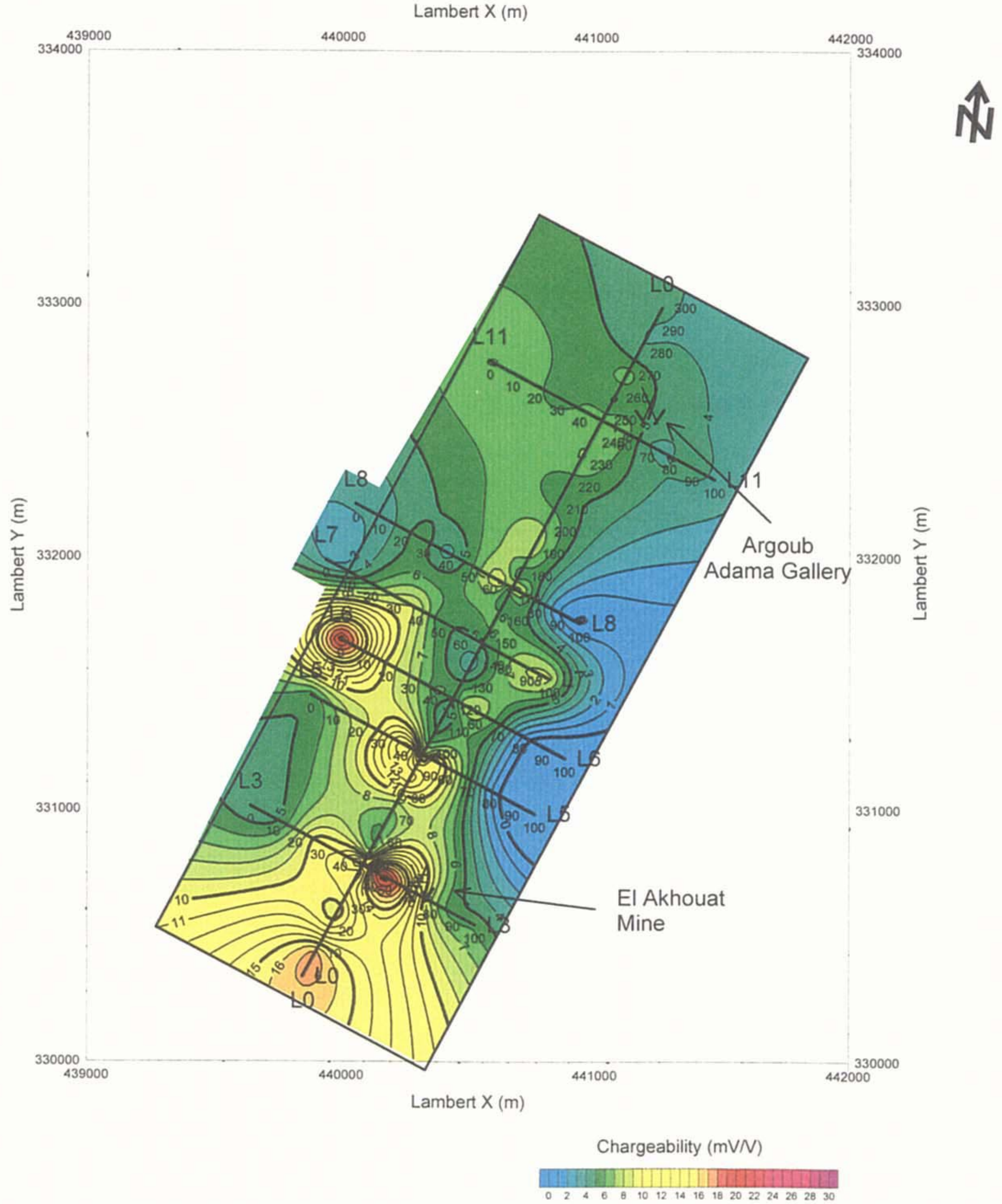

Legend

—— : IP survey Line

☐ : Survey Area

✕ : Closed Mine

Figure 125

Plan Map of Modeled Chargeability in El Akhouat - Argoub Adama area (Altitude: 400m)

Scale 1 : 25,000

March, 2000

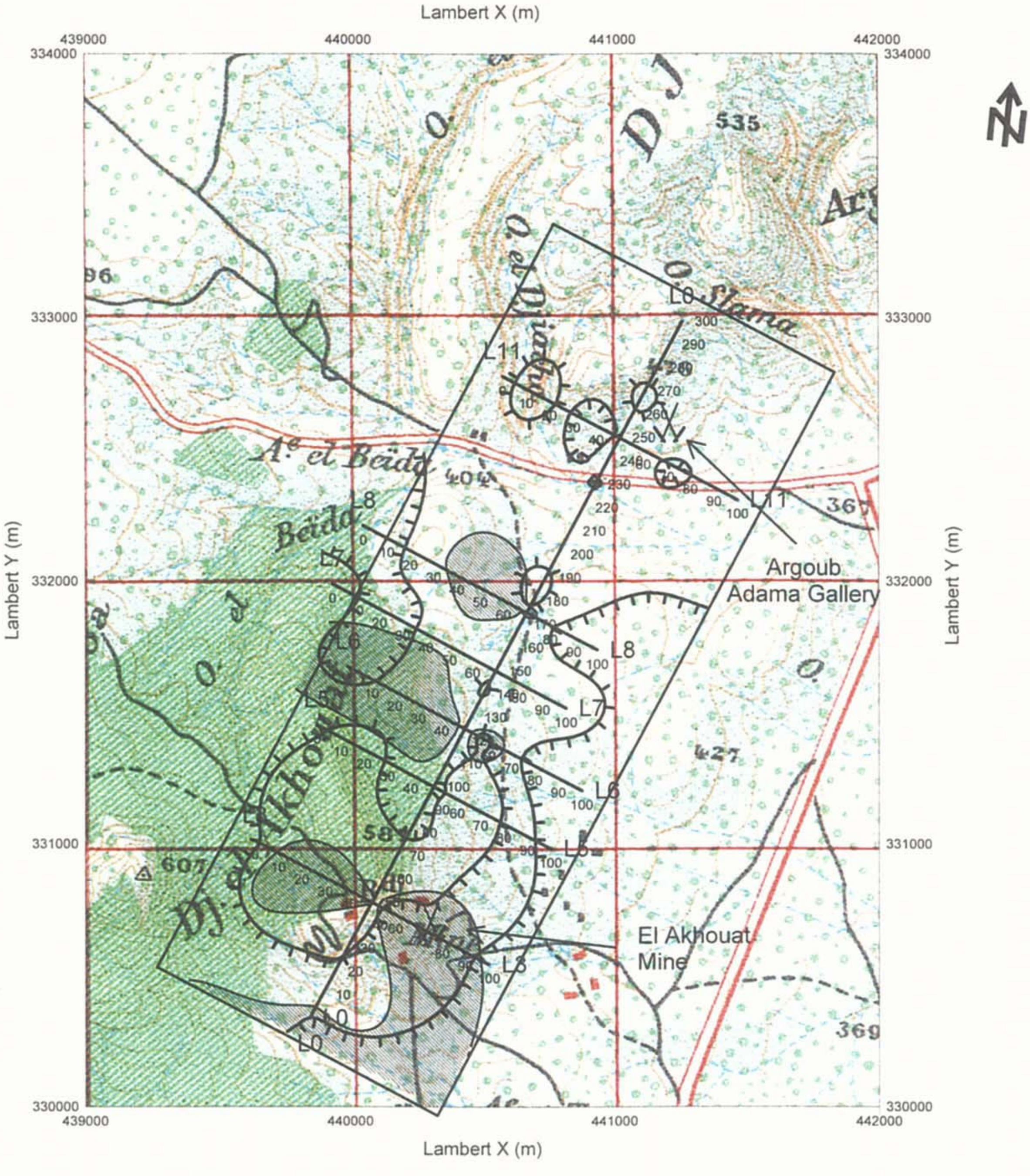

Legend

— : IP survey Line

☐ : Survey Area

: Closed Mine

Resistive zone > 100 Ω m (Altitude: 300m)

Conductive zone < 10 Ω m (Altitude: 300m)

High Chargeability < 10 mV/V (Altitude: 200m)

Figure 126

Interpreted IP survey map in El Akhouat - Argoub Adama area

Scale 1 : 25,000

March, 2000

resistivities. The old tunnel site of the Argoub Adama is situated around the resistivity discontinuity the same as the old mine site of the Bou Khil. However, the significant chargeability anomalies are not detected. The sedimentary rocks with low porosity and hardness are typical of Tertiary, which is distributed in the northern parts of the survey area and exhibits low resistivity.

Notwithstanding that the chargeability of zinc ore samples is less than 10 mV/V, high chargeability anomalies are widely distributed extending from the central to northern parts of the survey area. On the other hand, the lead sulfides are considered to give high chargeabilities and a little chalcopyrite, which exhibit high chargeability, are also recognized in this prospect area. However, a main causative factor of high chargeability is not specified. Phenomenally and qualitatively, the chargeability is just assumed to have relations with the mineralization.

The chargeability anomalies, which are detected at lower parts around stations from L6-0 to L0-125 and around station L0-175, are worthy of notice as the prospecting targets in the El Akhouat prospect, considering the pattern of resistivity distributions, locations of the chargeability anomaly and the high residual gravity anomalies.

4.3.4 Magnetic Survey

(1) Magnetic Total Intensity Map (Figure 127)

Magnetic total intensity in the prospect ranges between 1,162 and 4,145 nT, is the approximate average of 1,660 nT. In magnetic surveys carried out in middle latitude areas same as prospect, magnetic total intensity becomes higher in the south side of a magnetic anomalous structure, and lower in the north side of it. This section describes a distribution of magnetic total intensity anomaly higher than 2,000 nT.

There are a couple of small anomalies high in the north part of the prospect, for example near the L13-30. In the central part, two small anomalies high are located near the L9-70 and near the L6-80 in the east side, and an anomaly high is shown between the L7-0 and the L0-150 in the west side. Magnetic total intensity in the south part is higher than it in other parts. A big anomaly high is extended from the L4-70 to the L2-30 in the southwest part. The highest anomaly exceeding 4,000 nT is located near the L4-70, but there is no geological or artificial structure on the ground surface that make it high. It is possibly suggested that influences of houses and electric power lines cause an anomaly high between the L4-70 and the L4-90.

The El Akhouat mine is located in the vicinity of an anomaly high in the south part of the prospect. However, no valid magnetic characteristic is indicated near the Argoub Adama gallery.

The trend of magnetic total intensity higher in the southwest part is matched those of distributions of residual gravity and modeled resistivity. Because the extended directions of magnetic anomalies are different from those of them, it is difficult to discuss the relationship between magnetic property and other properties. Sedimentary rocks of which magnetic susceptibilities are less than those of volcanic rocks in general dominate the geology in prospect. Magnetic susceptibilities of the rock specimens measured in a laboratory are relatively small. It is supposed that magnetic susceptibility indicates contents of hematite and goethite in rocks of the prospect. But, the current data and information are not enough to relate the results of magnetic survey and laboratory test to known mineralizations and geology.

(2) Magnetic Profile (Figure 128)

Magnetic variation of every profile is shown on the magnetic profile. It is easier to recognize positions of magnetic total intensity peaks on this figure than on a magnetic total intensity map. Because it is difficult to relate the peaks to mineralization and geology in direct, the following characterizes magnetic total intensity variation on profiles from south to north.

Profile L2: There are three peaks beyond 2,000 nT near the L2-5, the L2-35 and the L2-60.

Profile L3: High magnetic total intensity of approximate 2,200 nT is extended between the L3-20 and L3-35, a peak of about 2,400 nT is located near the L3-55. It is supposed that the former links with the peaks near the L2-35 and the latter near the L2-60. The El Akhouat mine is located in the range of relatively high magnetic total intensity of approximate 2,000 nT.

Profile L4: There is the highest peak in the prospect exceeding 4,000 nT near the L4-5. Geology occurred the peak is not known, and the magnetic susceptibility of the rock specimen sampled near the peak is low of 0.00014 cgsemu/cm^3. Because there is also no artificial noise source near the anomaly, the cause of the anomaly is not distinguished. It is inferred that magnetic total intensity higher than 2,000 nT between the station L4-60 and the station L4-90 is occurred by artificial noise in the residence of the El Akhouat Mine.

Profile L5: Two peaks higher than 2,000 nT is located near the station L5-5 and the station L5-30. The former is linked with that near the station L4-5. Magnetic total intensity variation in the southeast part from the station L5-50 to the station L5-100 is little.

Profile L6: There are three peaks higher than 2,000 nT near the station L6-20, the station L6-60 and the station L6-80.

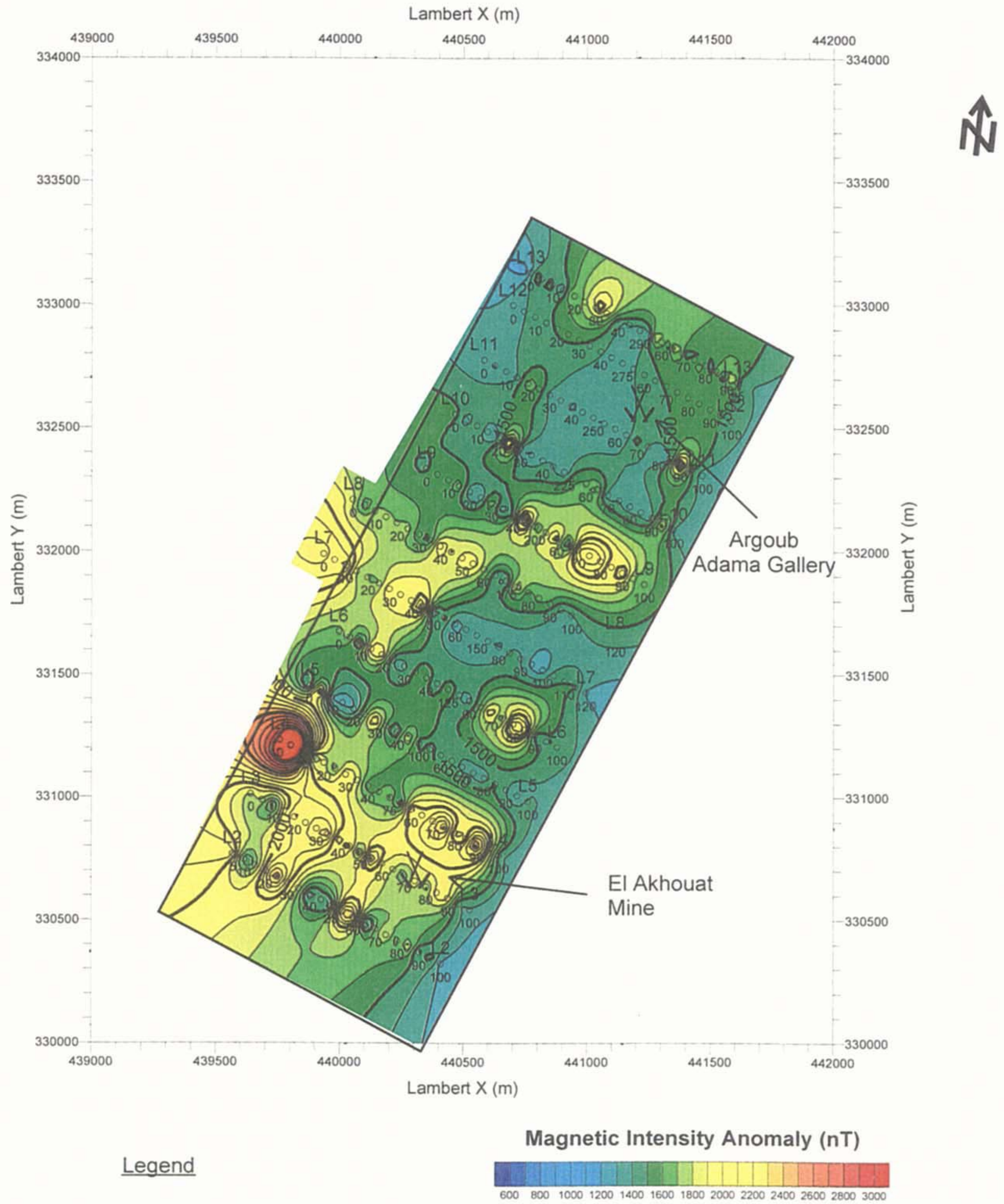

Legend

∘ : Magnetic Survey Station

□ : Survey Area

: Closed Mine

Figure 127

Magnetic Intensity Anomaly Map in El Akhouat - Argoub Adama area

Scale 1 : 25,000

March, 2000

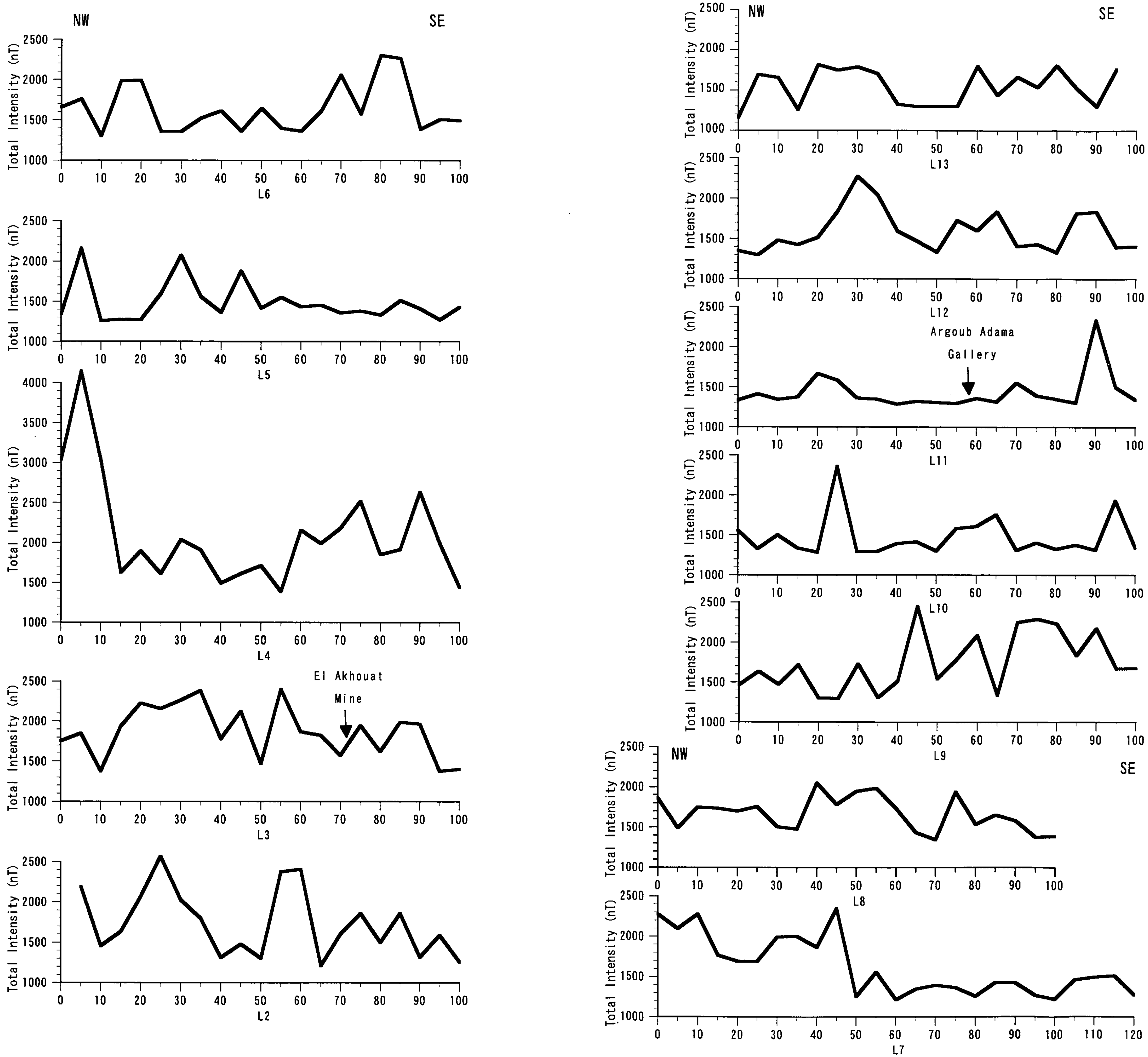

Figure 128

Profiles of Magnetic
Total·Intensity

Scale 1:10,000

Profile L7: High magnetic total intensity of about 2,000 nT is shown in the northwest part of the profile between the station L7-0 and the station L7-45. A peak of approximate 2,500 nT is located near the station L7-45. Other hand, magnetic total intensity between the station L7-0 and the station L7-45 is low of nearly 1,500 nT and its variation is relatively small.

Profile L8: Magnetic total intensity between the station L8-40 and the station L8-55 is high of nearly 2,000 nT. There is a peak of approximate 2,000 nT near the station L8-75.

Profile L9: There are four peaks near the station L9-45, between the station L9-70 and the station L9-80, near the station L9-60 and the station L9-90. The first is higher than 2,500 nT, the others is nearly 2,000 nT.

Profile L10: A peak of nearly 2,500 nT is located near the station L10-25. In the line setting, the hand of the compass did not indicate the north near the peak position. It is supposed that buried objects generate the peak.

Profile L11: There are two suggestions on a peak higher than 2,000 nT near the station L11-90. One is influence of an electric power line, and the other is relation with small peaks of the station L10-95, L12-90. There is no valid peak near the Argoub Adama gallery.

Profile L12: A broad peak higher than 2,000 nT is located near station L12-30.

Profile L13: Magnetic total intensity in almost the profile is low of nearly 1,500 nT.

(3) First Vertical Magnetic Derivative Map (Figure 129)

On the whole, variation of first vertical magnetic derivative in prospect is similar to that of magnetic total intensity. It is easier to distinguish small anomalies in the first vertical magnetic derivative map than in the magnetic total intensity map. Positive anomaly is distributed in the south part of prospect. Small peaks are laid in the anomaly. There is positive anomaly near the station L6-30 in the west part. Higher anomaly is extended in the approximately East-West direction from the station L7-0 to the station L9-100 in the central part. There are two positive anomaly belts. One extends toward the southwest, and the other towards the south. It is possible to relate the latter to the Triassic rocks.

The El Akhouat Mine is located in a high anomaly in the south part of the prospect. No valid magnetic anomaly is indicated near the Argoub Adama gallery.

(4)Cross Section Analysis

As stated above, magnetic structure was modeled simultaneous with gravity one. Magnetic total intensity is more sensitive than gravity in analyzing causative bodies. Therefore, Magnetic total intensity significantly contributed to fix shape of gravity and magnetic basement surfaces at cross section analysis. The gravity structure is principally two-layered, composed of a high density layer correlated to Createaceous limestone and underlying a low density gravity basement. An overlying high density layer is divided magnetic stripe structures. Because the surfaces of their basements were mentioned above, description on the stripe structures within overburdens is below.

①L-3 Cross Section (Figure 90)

Magnetic susceptibility of magnetic stripe structures in the upper layer ranging from 0.015 to 0.070 cgsemu/cm³ is relatively higher than common sedimentary rocks. Magnetic susceptibility of the stripe bodies in the both sides of basement rising in the southeastern part indicates 0.05 and 0.07 cgsemu/cm³ high particularly. It is possible that these high are correlated to mineralization because of their location in the vicinity of the old El Akhouat mine. However, magnetic susceptibility of the rock samples in and around the mine is low. The relationship between high susceptibility and mineralization is not specified yet.

②L-4 Cross Section (Figure 91)

Magnetic susceptibility of magnetic stripe structures in the upper layer ranging from 0.002 to 0.005 cgsemu/cm³ is less than the L-3 cross section. Although the highest peak exceeding 4,000 nT is indicated in the northwestern part, analyzed susceptibility is not so high as 0.005 cgsemu/cm³. Magnetic susceptibility of the stripe bodies in the both sides of basement rising in the southeastern part indicates higher than other bodies, same as L-3 cross section. Therefore, as mentioned above, the relationship between high susceptibility and mineralization is suggested. The susceptibility has possibility of a mineralization indicator in future.

③L-5 Cross Section (Figure 92)

Magnetic susceptibility of magnetic stripe structures in the upper layer ranging between 0.001 and 0.002 cgsemu/cm³ is still less than the L-4 cross section. The body in the vicinity of the basement rise near the station L5-70 has susceptibility of nearly 0. The body indicating a little higher susceptibility is located around the station L5-40 and identified high chargeability zone.

④L-6 Cross Section (Figure 93)

Magnetic susceptibility of magnetic stripe structures in the upper layer ranges from 0.002 and 0.003 cgsemu/cm³. The body overlying the rise of basement around the station L0-125 indicates susceptibility of nearly 0. High chargeability zone is distributed under the body of a little higher susceptibility of 0.002 cgsemu/cm³ in the northwestern part, while no valid chargeability is indicated around the body of 0.003

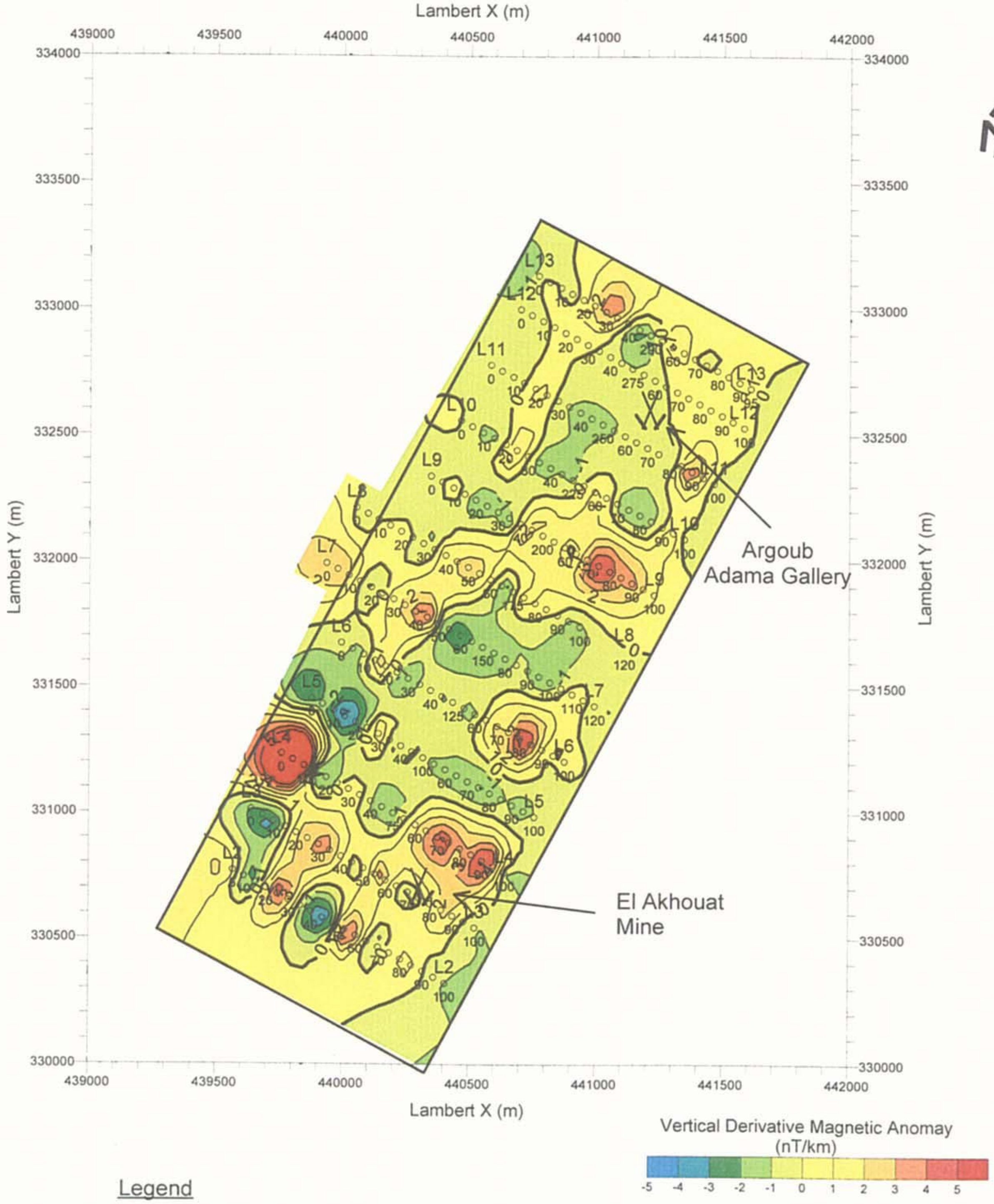

Legend

○ : Magnetic Survey Station

□ : Survey Area

: Closed Mine

Figure 129

Vertical Derivative Magnetic Anomaly Map in El Akhouat - Argoub Adama area

Scale 1 : 25,000

March, 2000

cgsemu/cm^3 between the station L6-70 and -80.

⑤L-7 Cross Section (Figure 94)

Magnetic stripe structures in the upper layer indicate susceptibility ranging from 0.002 and 0.005 cgsemu/cm^3. The small body indicating susceptibility of 0.005 cgsemu/cm^3 overlies the rise of basement around the station L7-40 in the central part.

⑥L-8 Cross Section (Figure 95)

Magnetic stripe structures in the upper layer indicate susceptibility ranging from 0.001 and 0.003 cgsemu/cm^3. The bodies in the both sides of the rise of basement around the station L0-175 in the central part indicate susceptibility of 0.003 cgsemu/cm^3. The chargeability zone higher than 10 mV/V is extended around two rises of basement.

⑦L-11 Cross Section (Figure 96)

There is only one body of around the station L11-80 in the southeastern part. No valid magnetic body is indicated in the vicinity of the Argoub Adama gallery.

(5) Interpreted Magnetism Map

The basement rises resulted from simultaneous gravity and magnetic cross section analysis are superimposed over the magnetic total intensity higher than 2,000 nT as shown Figure 130. Many magnetic anomalies higher than 2,000 nT are distributed from the central part to the south part involved the El Akhouat mine. Although it is suggested that high magnetic zones are related to the classification of Cretaceous limestone, it is difficult to prove the fact clearly. Magnetic characteristics are little correlation to that resulted from gravity and IP survey. It is supposed that distribution of magnetic total intensity is affected the difference of contents of magnetic minerals like as hematite and goethite.

However, it is supposed that the basement rises resulted from the gravity and magnetic cross section analysis have correlation to narrow Triassic system extended from north to south. Basements on the cross sections L3, L4 and L8 rise like peak, while those on the cross sections L5 and L6 are outlined steps rising in the southeastern side. The step structures are identified jutting out towards the northwest of outcropped basements in the southeastern ends on the cross sections L3, L4 and L8.

4.3.5 Laboratory Tests

(1) Measurement of Rock density

Enforced wet densities of 19 rock samples collected in and around the El Akhouat - Argoub Adama prospect are resulted in the range from 2.26 through 3.72 g/cm^3 from density measurement in laboratory. The estimated average density of 2.68

g/cm^3 is higher than the correction density of 2.33 g/cm^3 adopted in the current gravity survey, same as the Bou Khil prospect. The fact may be explained from the reasons why samples include two extreme heavy samples and the five sixths of samples indicate less porosity than 10 %. Average density of rock samples decreases in order of the Cretaceous system of 2.79 g/cm^3, the Triassic system of 2.59 g/cm^3 and the Tertiary system of 2.56 g/cm^3. The highest average density of 2.92 g/cm^3 is indicated in the rocks collected in the transition zone around the ore deposits.

(2) Measurement of Resistivity and Chargeability

The results from resistivity and chargeability measurement of 18 rock samples measured density, except for a sample disintegrated during immersion, are shown in Table 32. Resistivities ranging from 167 to 14,591 Ωm are higher than the measured resistivities from the field survey, ranging from several tens through several hundreds Ωm, same as the case of the Bou Khil prospect. The different results between from the laboratory test and the field IP survey is not explained enough that porosity of samples is less than one of rocks distributed in the prospect. It is supposed that low resistivity in the field is affected due to conductive pore water.

In the case of field IP survey chargeability measured in the prospect is higher than it in the Bou Khil prospect. On the contrary, maximum chargeability of around 9 mV/V resulted from measurement of samples collected in the prospect is indicated lower than that in the Bou Khil prospect. Low chargeability of 2.2 nd 4.5 mV/V are measured from the vein samples of no. 16 and 17 collected at the outcrop in the old El Akhouat working. Even zinc ore indicates chargeability less than 1 mV/V. The results of the current laboratory test cannot specified the reason why chargeability is generated in the prospect. It is expected that sulfide lead minerals like a galena generate it on the basis of the laboratory test result for the Bou Khil prospect.

(3) Measurement of Magnetic Susceptibility

Magnetic susceptibility of 31 samples, ranging from 0.001 to 0.006 cgsemu/cm^3 and averaging 0.0024 cgsemu/cm^3, is as low as analyzed one from the magnetic field survey. Almost estimated samples are sedimentary rocks. In general, they indicate magnetic susceptibility lower than volcanic rocks due to less contents of magnetic minerals.

No valid difference of magnetic susceptibility according to various kinds of geology and rock is recognized. No local characterization is indicated, too. Therefore, the results of laboratory magnetic susceptibility measurement are not enough to estimate magnetic anomalies in the prospect.

(4) Measurement of Natural Magnetic Remnant

Natural magnetic remnant of 10 samples is estimated. The sample no. 11

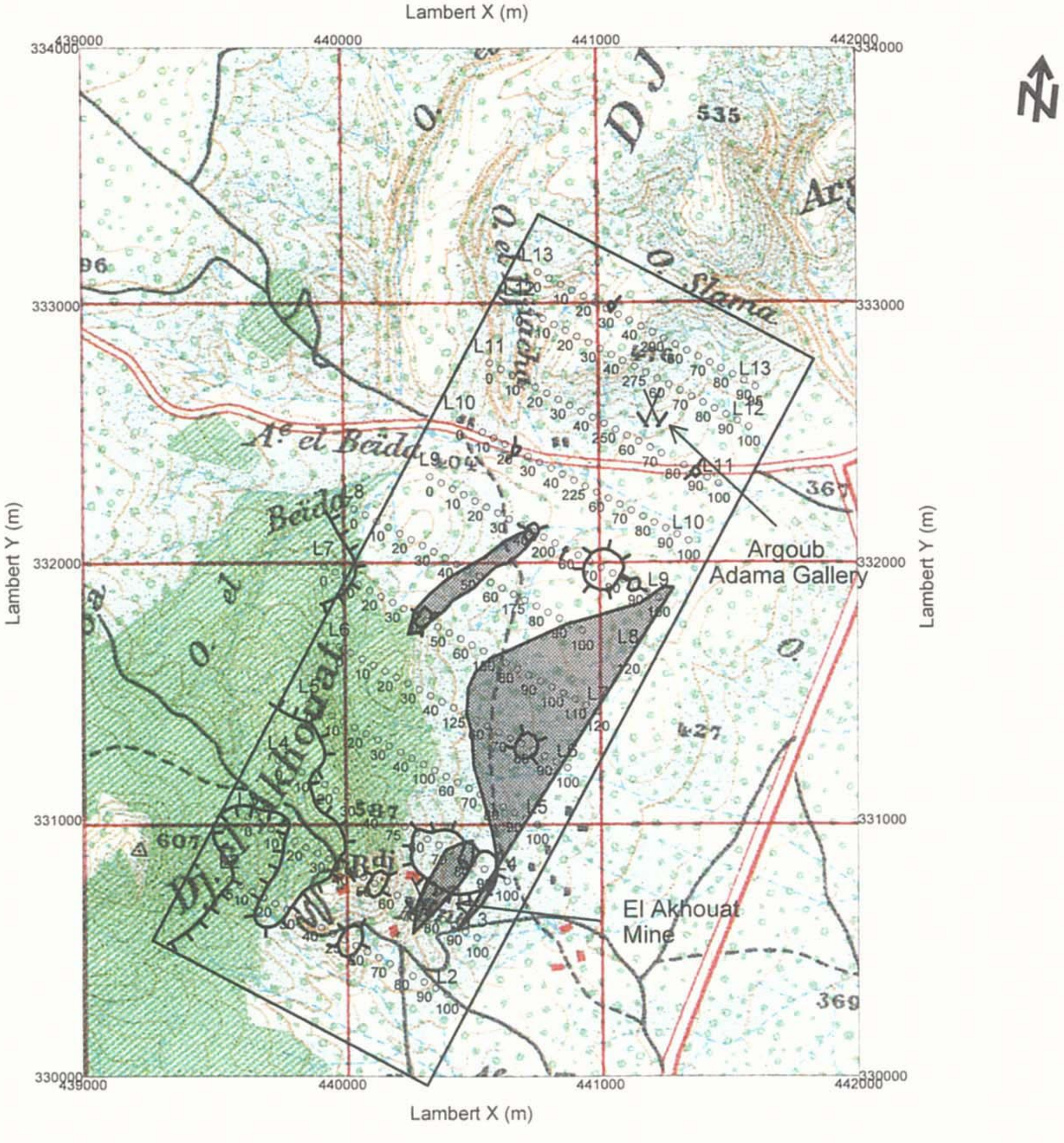

Legend

- ○ : Magnetic Survey Station
- □ : Survey Area
- ⚒ : Closed Mine
- High Magneticl Anomaly > 2000 nTI
- Interpreted Shallow Basement

Figure 130

Interpreted Magnetism Map in El Akhouat - Argoub Adama area

Scale 1 : 25,000

March, 2000

shows natural magnetic remnant same as present geomagnetism. Natural magnetic remnant of samples is not classified according to geology and rock, but those of samples collected within close outcrops is similar to each other. The sample no. 1 and 2 collected around the El Akhouat workings indicate similar natural magnetic remnant except for declination, their Königsberger ratio expressed as Q are high. The samples from no. 8 to no. 10 collected in the north part of the prospect indicate negative susceptibility, similar intensity of residual magnetism. Declination and inclination of the sample no. 8 became similar value after demagnetization. The negative susceptibility reflects diamagnetic carbonate minerals. The fact that the sample no. 8 keeps strong residual magnetism after demagnetization suggests hematite as a magnetic mineral.

The Königsberger ratio of almost samples is so small that Natural magnetic remnant may not be considered significantly in analysis of the current magnetic survey. High susceptibility of some limestone samples proves striped magnetic structures resulted from the current survey.

Table 31 Results of Rock Density measurement of specimens in El Akhouat area

No.	Location	Geology	Rock	Weight (g)				Density (g/cm³)			Porosity (%)
				W1	W2	W3	W4	Natural	Dry	Wet	
1	L11-40	Trias	Dolomite	80.10	46.90	75.80	75.70	2.28	2.28	2.41	13.3
2	L11-30	〃	Lime Stone	160.40	98.80	159.65	159.50	2.59	2.59	2.60	1.5
3	L11-20	〃	〃	165.55	105.35	165.15	164.85	2.74	2.74	2.75	1.2
4	L4-30	Cretacious	Lime Stone	147.75	88.00	141.85	141.30	2.37	2.36	2.47	10.8
5	L4-0	〃	〃	162.90	100.10	159.35	158.60	2.54	2.53	2.59	6.8
6	L3-60	〃	〃	140.30	87.10	138.50	138.30	2.60	2.60	2.64	3.8
7	L3-25	〃	〃	98.65	59.85	95.70	95.10	2.47	2.45	2.54	9.1
8	L0-25	〃	〃	168.80	105.60	168.00	167.80	2.66	2.66	2.67	1.6
9	L0-5L0	〃	〃	164.05	101.60	161.95	161.30	2.59	2.58	2.63	4.4
10	L0-170	〃	〃	200.00	135.65	199.10	198.85	3.09	3.09	3.11	1.8
11	L3-75	〃	〃	159.10	99.10	157.90	157.20	2.63	2.62	2.65	3.2
12	L8-60	〃	〃	87.50	54.75	86.85	86.65	2.65	2.65	2.67	2.6
13	L0-260	〃	〃	168.85	105.40	167.35	166.85	2.64	2.63	2.66	3.2
14	L11-60	Tertiary	Conglomarate	160.80	97.90	157.75	156.65	2.51	2.49	2.56	6.6
15	L11-50	Quarternary	Calcalious Conglomarate	108.60	60.55	99.95	99.25	2.08	2.07	2.26	19.5
16	L3-70	Transition	Vein	169.75	107.45	167.35	165.25	2.69	2.65	2.72	7.2
17	〃	〃	〃	246.10	179.95	245.75	245.50	3.72	3.71	3.72	0.9
18	〃	〃	〃	263.85	162.90	262.25	261.85	2.60	2.59	2.61	2.0
19	L0-260	〃	〃	135.75	84.15	131.65	130.80	2.55	2.53	2.63	9.6

Table 32 Results of IP measurement of specimens in El Akhouat area

No.	Location	Geology	Rock	Diameter (mm)	Length (mm)	Current (μA)	Voltage (V)	Resistivity (Ωm)	Chargeability (mV/V)
1	L11-40	Trias	Dolomite	716.38	50.2	5	0.1996	570	0.99
2	L11-30	〃	Lime Stone	35.00	65.30	5	1.7588	5,183	0.99
3	L11-20	〃	〃	35.40	61.50	5	4.5588	14,592	8.96
4	L4-30	Cretacious	Lime Stone	35.55	61.55	5	0.1027	331	3.20
5	L4-0	〃	〃	35.35	64.55	5	0.0605	184	2.68
6	L3-60	〃	〃	35.50	54.40	5	0.3425	1,246	0.88
7	L3-25	〃	〃	35.00	41.00	5	0.0357	167	2.60
8	L0-25	〃	〃	35.50	65.00	5	0.8561	2,607	1.68
9	L0-5	〃	〃	35.35	65.35	5	0.8415	2,528	2.25
10	L0-170	〃	〃	35.45	65.80	5	2.0611	6,183	2.97
11	L3-75	〃	〃	35.20	63.30	5	0.2917	897	4.11
12	L8-60	〃	〃	35.50	34.10	5	1.7797	10,332	2.15
13	L0-260	〃	〃	35.10	66.10	5	0.0877	257	2.76
14	L11-60	Tertiary	Conglomarate	35.30	65.10	5	0.2003	602	5.86
15	L11-50	Quarternary	Calcalious Conglomarate	35.50	49.70	5	0.0771	307	5.31
16	L3-70	Transition	Vein	34.75	66.70	5	0.4459	1,268	4.43
17	〃	〃	〃	35.50	67.30	5	1.9858	5,841	2.22
19	L0-260	〃	〃	34.60	55.40	5	0.5863	1,990	3.98
20	L3-70	〃	Zn Ore			5	1.1155		0.87

Table 33 Results of magnetic susceptibility measurement of specimens in El Akhouat area

No.	Geology	Rock	Location	Weight (g)	Diameter (mm)	Density (g/cm^3)	Porosity (%)	Susceptibility (cgsemu/ cm^3)
1	Triassic	Dolomite	L6-25	82.65	24.50	2.61	2.5	0.00305
2	Triassic	Dolomite	L11-35	80.30	24.50	2.39	7.4	0.00279
3	Triassic	Dolomite	L11-30	85.40	24.50	2.51	5.7	0.00258
4	Triassic	Dolomite	L11-25	68.35	24.50	2.10	12.2	0.00188
5	Triassic	Dolomite	L12-40	87.05	24.50	2.48	9.7	0.00294
6	Cretaceous	Limestone	L3-75	89.25	24.50	2.81	8.3	0.00188
7	Cretaceous	Limestone	L3-70	83.90	24.50	2.42	8.7	0.00188
8	Cretaceous	Limestone	L4-55	93.85	24.50	2.58	4.4	0.00142
9	Cretaceous	Limestone	L5-45	94.60	24.50	2.62	3.0	0.00155
10	Cretaceous	Limestone	L6-20	91.60	24.50	2.56	4.3	0.00243
11	Cretaceous	Limestone	L6-30	82.70	24.50	2.45	7.9	0.00296
12	Cretaceous	Limestone	L8-35	99.45	24.50	2.71	6.3	0.00524
13	Cretaceous	Limestone	L8-15	91.80	24.50	2.58	5.3	0.00174
14	Cretaceous	Limestone	L8-30	95.30	24.50	2.68	1.0	0.00199
15	Cretaceous	Limestone	L10-30	86.35	24.50	2.43	8.6	0.00125
16	Cretaceous	Limestone	L11-25	94.90	24.50	2.76	1.7	0.00204
17	Cretaceous	Limestone	L12-30	97.75	24.50	2.75	3.1	0.00222
18	Cretaceous	Limestone	L12-25	98.10	24.50	2.77	0.8	0.00217
19	Cretaceous	Limestone	L12-70	90.60	24.50	2.72	2.0	0.00190
20	Tertiary	Conglomerate	L11-55	85.60	24.50	2.43	7.1	0.00262
21	Tertiary	Limestone	L11-45	96.70	24.50	2.66	1.9	0.00179
22	Tertiary	Limestone	L11-50	95.00	24.50	2.70	1.7	0.00193
23	Tertiary	Limestone	L12-35	96.10	24.50	2.69	1.1	0.00138
24	Tertiary	Limestone	L12-20	90.00	24.50	2.60	3.8	0.00413
25	Tertiary	Sandstone	L11-40	72.40	24.50	2.35	19.7	0.00268
26	Tertiary	Sandstone	L12-65	87.15	24.50	2.49	3.3	0.00178
27	Quaternary	Conglomerate	L7-35	60.45	24.50	2.02	23.5	0.00618
28	Quaternary	Conglomerate	L11-20	85.65	24.50	2.68	6.3	0.00271
29	Quaternary	Conglomerate	L12-55	90.00	24.50	2.68	1.5	0.00164
30	Quaternary	Limestone	L0-245	93.00	24.50	2.65	1.1	0.00127
31	Quaternary	Limestone	L12-50	88.70	24.50	2.66	2.1	0.00161
32	Quaternary	Limestone	L12-60	84.75	24.50	2.65	1.3	0.00192

Table 34 Results of Natural Remanent Magnetism of specimens in El Akhouat area

No.	Geology	Rock	Location	Weight (g)	Length (mm)	Diameter (mm)	Susceptibility (cgsemu/cc)	Declination (°)	Inclination (°)	(A/m)	Q
1	Triassic	Dolomite	L3-75	29.77	23.55	24.65	0.00215	7	34	6.99E-3	7.072
2	Cretaceous	Limestone	L3-70	25.48	22.95	24.65	0.00100	255	49	3.65E-3	7.955
3	Cretaceous	Limestone	L5-45	27.22	22.95	24.65	0.00199	23	40	7.77E-5	0.085
4	Cretaceous	Limestone	L6-20	26.78	21.80	24.65	0.00271	3	12	5.98E-4	0.479
5	Cretaceous	Limestone	L6-30	26.09	22.00	24.70	0.00234	1	22	4.36E-5	0.041
6	Cretaceous	Limestone	L8-35	27.61	22.00	24.65	0.02515	322	34	7.51E-3	0.649
7	Cretaceous	Limestone	L8-30	27.23	21.60	24.65	0.00639	14	61	2.69E-2	9.162
8	Tertiary	Limestone	L0-245	26.91	22.25	24.40	-0.00063	116	39	3.76E-3	-12.944
9	Tertiary	Limestone	L11-45	27.92	22.25	24.40	-0.00058	226	-48	3.80E-3	-14.145
10	Quaternary	Conglomerate	L12-70	29.31	22.30	24.55	-0.00058	225	46	3.62E-3	-13.475
11	Quaternary	Talus	L4-55	23.22	22.30	24.30	0.01056	354	52	4.53E-3	0.932